CELLULAR AUTOMATA AND MARKOV CHAIN MODELLING FOR PREDICTION OF FUTURE LULC: A CASE STUDY OF DODDAHALLA WATERSHED IN SOUTHERN KARNATAKA

Thesis

Submitted to the

G. B. Pant University of Agriculture and Technology
Pantnagar- 263145, Uttarakhand, India

By

Dheerajkumar Sidalingappa Hanamapure
Id. No. 58198

IN PARTIAL FULFILLMENT OF THE REQUIREMENTS FOR THE DEGREE OF

Master of Technology
in
Agricultural Engineering

(Soil and Water Conservation Engineering)

July, 2023

ACKNOWLEDGEMENT

My sincere gratitude goes to God for his perennial guidance and protection to complete the task. First and foremost, I thank my Advisor and Chairman, Advisory Committee, **Dr. Pankaj Kumar**, Associate Professor, Department of Soil and Water Conservation Engineering, G.B.P.U.A & T, Pantnagar. Words are inadequate to express my sincere and deepest feelings of gratitude originating from the innermost core of my heart for his benevolent guidance, wholehearted encouragement, and for all the trust he had in my ability responsible for the present accomplishment.

I would like to thank my advisory committee members, **Dr. Devendra Kumar,** Professor, Department of Soil and Water Conservation Engineering, **Dr. H. J. Shiva Prasad,** Professor, Department of Civil Engineering, **Dr. Dheeraj Kumar**, Associate professor, Dept. of Irrigation and Drainage Engineering for giving their valuable suggestions and help at various stages of the research work.

I wish to express my sincere gratitude to **Dr. Anil Kumar,** Professor & Head, Department of Soil and Water Conservation Engineering, for their guidance and valuable suggestions. My inexplicable gratitude goes to **Dr. Alaknanda Ashok**, Dean College of Technology, **Dr. Kiran P. Raverkar**, Dean, College of Post Graduate Studies and for extending all the necessary help and providing facilities for the study. I express my sincere thanks to **Dr. Anil Kumar**, H.O.D, **Dr. Pravendra Kumar**, Professor, **Dr. P.V. Singh**, S.R.O., **Dr. Deepak Kumar** Assistant Professor Department of Soil and Water Conservation Engineering and for their valuable advice and constructive suggestions.

I wish to place on record my appreciation and sincere thanks to the office staff of Soil and Water Conservation Engineering Mr. Sageer, Yadav Ji, Shinu mam and Rashmi mam. I am grateful to my well-wisher Ms. Tithi Dutta and senior Nikhil sir, Himadri mam, Rajat sir, Yogesh Kumar sir, Priya mam and Aekesh sir for their help and support during my study and research work. I thank my friends, Pinki, Ankita, Shashi, Soumya, Akash, Pawan, Sanjay, Vineet, Milind, Pradeep and Prabhu for their wholehearted help and timely motivation. I am grateful to all my colleagues and juniors for their help during research work.

I would like to avail this opportunity to express my heartiest sense of reverence and immense love to my lovely parents Mr. Sidalingappa H and Mrs. Parvati H and to my elder sister Mrs. Poornima T. for their everlasting love, benediction, and support. At last, I would like to remember the “Lord Shiva” who has given me strength and perseverance to complete this assignment.

Pantnagar
July, 2023

(Dheerajkumar Sidalingappa Hanamapure)
Author

CERTIFICATE-I

This is to certify that the thesis entitled **“Cellular Automata and Markov Chain Modelling for Prediction of Future LULC: A Case Study of Doddahalla Watershed in Southern Karnataka”** submitted in partial fulfillment of the requirements for the degree **Master of Technology** in **Agricultural Engineering** with major **Soil and Water Conservation Engineering**, of the College of Post-Graduate Studies, G. B. Pant University of Agriculture and Technology, Pantnagar , is a record of bonafide research carried out by **Mr. Dheerajkumar Sidalingappa Hanamapure,** Id. No. **58198,** under my supervision and no part of the thesis has been submitted for any other degree or diploma.

The assistance and help received during the course of this investigation have been acknowledged.

Pantnagar
July, 2023

(Pankaj Kumar)
Chairman
Advisory Committee

CERTIFICATE-II

We, the undersigned, members of the Advisory Committee **Mr. Dheerajkumar Sidalingappa Hanamapure,** Id. No. **58198,** a candidate for the **Master of Technology** in **Agricultural Engineering** with major **Soil and Water Conservation Engineering**, agree that the thesis entitled **"Cellular Automata and Markov Chain Modelling for Prediction of Future LULC: A Case Study of Doddahalla Watershed in Southern Karnataka"** may be submitted in partial fulfillment of the requirements for the degree.

(Pankaj Kumar)
Chairman
Advisory Committee

(Devendra Kumar)	**(H. J. Shiva Prasad)**	**(Dheeraj Kumar)**
Member	Member	Member

CONTENTS

Sl. No.	CHAPTER		PAGE No.
	LIST OF TABLES		
	LIST OF FIGURES		
	LIST OF SYMBOLS		
	LIST OF ABBREVIATIONS		
1.	**INTRODUCTION**		**1-3**
2.	**REVIEW OF LITERATURE**		**4-24**
3.	**MATERIALS AND METHODS**		**25-44**
	3.1	Study Area Description	25
	3.2	Data Collection and pre-processing	26
		3.2.1 Remote sensing data for LULC assessment	27
	3.3	Image classification	28
		3.3.1 Maximum Likelihood Classification	29
	3.4	Accuracy Assessment	31
		3.4.1 Overall Accuracy	31
		3.4.2 Producer Accuracy	31
		3.4.3 Kappa Coefficient	32
	3.5	Prediction of LULC change with CA Markov	32
		3.5.1 Land Change Modeler (LCM)	33
		3.5.2 Cellular Automata Approach	34
	3.6	Prediction of Future LULC Dynamics	36
		3.6.1 Analysis on dynamic change rate of land use	36
		3.6.2 Transition Probabilities	37
		3.6.3 Model Validation	38
	3.7	Indices for LULC Assessment	41
		3.7.1 Normalized Difference Vegetation Index (NDVI)	41
		3.7.2 Normalized Difference Built-up Index (NDBI)	42

	3.7.3	Normalized Difference Water Index (NDWI)	43
4.	**RESULTS AND DISCUSSION**		**45-65**
	4.1	Generation of Land use and Land cover (LULC) Map	45
	4.2	Temporal Changes in Land Use and Land Cover Class Map	46
	4.2.1	Forest Area	48
	4.2.2	Agricultural land	48
	4.2.3	Fallow land	49
	4.2.4	Built up area	50
	4.2.5	Water	51
	4.2.6	Barren Land	52
	4.3	Key Drivers used for Prediction of LULC for the year 2033	53
	4.4	Simulation of LULC Change Using Markov Chain Analysis (CA-Markov) Model	55
	4.5	Land use and land cover prediction	56
	4.5.1	Gains and Losses occurred in LULC	58
	4.5.2	Parameters and Performances of the Model	59
	4.6	Validation of Model	59
	4.7	Indices for LULC Model Change Assessment	60
	4.7.1	Temporal Analysis of Builtup Development Using NDBI	60
	4.7.2	Temporal Analysis of Vegetation using NDVI	62
	4.7.3	NDWI-Based Temporal Analysis of Water Bodies	63
	4.8	Kappa accuracy	64
5.	**SUMMARY AND CONCLUSION**		**66-69**
	LITERATURE CITED		
	CURRICULUM VITA		
	ABSTRACT (English)		
	ABSTRACT (Hindi)		

LIST OF TABLES

Table No.	Title	Page No.
3.1	Descriptive Table of Landsat 7 and 8 Satellite Characteristics	27
3.2	Details of the LULC Data Set for each decade.	29
3.3	Landsat 7 band classification	30
3.4	Landsat 8 band classification	30
3.5	Thematic Bands of LANDSAT Satellite	42
4.1	Characteristics of land cover classes	45
4.2	Transition matrix of future LULC prediction for year 2033	56

LIST OF FIGURES

Figure No.	Title	Page No.
3.1	Location Map of Doddahalla Watershed of Chitradurga District in Karnataka	25
3.2	Methodological scheme for LULC classification and future LULC prediction	39
3.3	Flow Chart of the Modelling Process	40
4.1	Temporal Analysis of Land Use and Land Cover from 2003-2033	47
4.2	Decadal variation in Land Use of the Doddahalla Watershed	47
4.3	Variation in area of forest area during the period from 2003-2023	48
4.4	Variation in area of Agriculture land during the period from 2003-2023	49
4.5	Variation in area of fallow land during the period from 2003-2023	50
4.6	Variation in area of Built-up land during the period from 2003-2023	51
4.7	Variation in area of water during the period from 2003-2023	52
4.8	Variation in area of Barren land during the period from 2003-2023	53
4.9	Map of Drivers Used prediction of future LULC	55
4.10	Simulated LULC map for the year 2023	56
4.11	Predicted LULC map for year 2033	57
4.12	Temporal Variation of NDBI Maps of 2003, 2013, and 2023	61
4.13	Temporal Variation of NDVI Maps of 2003, 2013, and 2023	63
4.14	Temporal Variation of NDWI Maps of 2003, 2013, and 2023	64
4.15	Graph Representing Kappa Accuracy	65

LIST OF ABBREVIATIONS

DEM	:	Digital Elevation Model
et al	:	And others
Fig.	:	Figure
GIS	:	Geographic Information System
LULC	:	Land Use Land Cover
NASA	:	National Aeronautics and Space Administration
QGIS	:	Quantum Geographic Information System
RS	:	Remote Sensing
SRTM	:	Shuttle Radar Topography Mission
UTM	:	Universal Transverse Mercator
viz.	:	Namely
WGS	:	World Geodetic System
NDVI	:	Normalized Difference Vegetation Index
NDBI	:	Normalized Difference Built-up Index
NDWI	:	Normalized Difference Water Index
MLC	:	Maximum Likelihood Classification
Kappa	:	Cohen's Kappa Coefficient
ROI	:	Region of Interest
IRS	:	Indian Remote Sensing
FCC	:	False Colour Composite
MSL	:	Mean Sea Level
MXL	:	Maximum Likelihood
SWIR	:	Short-wave Infrared
NIR	:	Near Infrared
A	:	Area

ha-m	:	Hectare meter
km	:	Kilometer
km^2	:	Square kilometer
m	:	Meter
Sl	:	Slope
m	:	Meter
mm	:	Millimeter

LIST OF SYMBOLS

'	:	Minute
"	:	Second
%	:	Percent
/	:	Per
<	:	Less than
>	:	Greater than
$\geq$	:	Greater than equal to
Σ	:	Summation
$\aleph$	:	Aleph

Introduction

Chapter 1 INTRODUCTION

Information from land use and land cover is crucial for modelling and comprehending many Earth surface processes **(Jia *et al*., 2014)**. It is crucial to record regional changes in land use and land cover (LULC) since this information provides atmospheric as well as environmental climate change studies **(Grecchi *et al*., 2014)**. The study and depiction of the intricate relationships between human activity and the environment, sustainable development strategies and spatial planning can all benefit from the identification and measurement of spatiotemporal variations in LULC **(Disperati *et al*., 2015)**. In order to manage watersheds and increase agriculture related output, the information on the current land cover is crucial. The climate, ecological health, and socioeconomic needs are some of the interconnected variables, result in changes in land cover. Land usage is the area that is used by human activities, while land cover is the combination of biotic and abiotic elements of the Earth system. For the communities, living particularly in drylands, vegetation is the vital source of food and income. They rely on it for grazing for their animals, food, and fire wood **(Ibrahim *et al*., 2015)**.

Data from remote sensing systems has shown to be a useful and effective tool for tracking changes in vegetation. It offers in-depth, accurate, objective and comprehensible information about the spatial variability of the land surface **(Jia *et al*., 2014; Rulinda *et al*., 2012)**. Landsat satellite outputs are well-known and often used for mapping and exploring a diversity of Earth resources, particularly those classified under the LULC system **(Omuto *et al*., 2010)**. Land use land cover (LULC) maps are like treasure maps for natural resource management, guiding us through the vast and complex landscape to uncover hidden gems and avoid dangerous pitfalls **(Rawat *et al*., 2013)**. Without them, we face the risk of losing priceless resources like water, soil, and vegetation as well as the biodiversity and ecosystem services that keep us alive**.** Unfortunately, rapid and intense changes in LULC pose a significant threat to our natural reserves, locally, regionally, and nationally **(Twisa *et al*., 2019)**. To monitor and understand these changes, we rely on diachronic LULC maps and time-series of remote sensing (RS) data, which allow us to track the evolution of the landscape over time and across space **(Fichera *et al*., 2012)**, accounting for subtle gradients and variations **(Vizzari *et al*., 2012)**.

At the heart of LULC mapping lies the use of satellite imagery, such as that provided by the Landsat Imageries. This state-of-the-art imaging system produces high-quality RS data that are consistent with earlier Landsat missions, enabling us to track changes over multi-decadal periods. Multispectral satellite images and their bands are the great source of data for LULC classification. **(Irons *et al*., 2012)**. To classify LULC, various approaches can be used, such as pixel or object-based discrimination, with the latter being increasingly popular thanks to Geographic Object-Based Image Analysis (GEOBIA). GEOBIA allows for the segmentation and classification of objects at different scales improving the accuracy and reliability of LULC classification **(Blaschke *et al*., 2010)**. Object identification is performed by clustering similar pixels into image clusters and converting them into vectors **(Solano *et al*., 2019)**. Subsequent analysis of texture and context information is then used to perform the final object classification. However, GEOBIA methods require significant computational and storage resources, particularly for high-resolution images **(Flanders *et al*., 2020)**.

The prediction of LULC is of major importance in understanding and handling the ever-changing variations in the Earth's surface. The CA-Markov model has been identified as a viable method for predicting land use and land cover (LULC) changes. This approach is based on the integration of cellular automata (CA) and Markov chain principles, which enables the simulation and prediction of LULC changes. The utilisation of the CA-Markov model involves the incorporation of spatial attributes of land use alterations through the partitioning of the research region into individualised cells or pixels, signifying distinct land use classifications. The model's cellular automata component specifies the transition rules at the cell level, which are determined by the land use types of adjacent cells. This approach captures the local dynamics of land use change. The incorporation of transition probabilities that denote the probability of land use conversion from one category to another is a manifestation of the Markov chain aspect. Through the iterative application of rules and probabilities, the CA-Markov model is capable of simulating spatial-temporal changes in land use and generating future projections **(Liu *et al.*, 2017)**.

The utilisation of an integrated modelling approach presents numerous benefits for the prediction of land use and land cover (LULC). The methodology captures the spatial patterns and surrounding interactions, thereby facilitating the integration of local context and spatial interactions. The model incorporates temporal considerations by incorporating historical land use changes through the Markov chain, resulting in a dynamic portrayal of land use dynamics. The CA-Markov model is a useful instrument for comprehending and predicting land use transformations, which can aid policymakers, urban planners, and researchers in making informed decisions concerning sustainable land management and resource allocation **(He *et al.*, 2018)**.

The current study concentrates on creating historical and current LULC maps for the Doddahalla watershed in southern Karnataka, and then application of CA Markov model to predict future LULC change. The study's objectives are as follows:

i. To delineate the Doddahalla watershed using remote sensing and GIS techniques,

ii. To prepare the LULC maps for the years 2003, 2013 and 2023 for the study region,

iii. To predict the future LULC by CA Markov model for the year 2033 using past and present LULC of the study region,

iv. Comparison among past, present and future LULC maps and analysis of change detection in the study region.

Review of Literature

Chapter 2 REVIEW OF LITERATURE

This chapter deals with the earlier work done on LULC mapping using remote sensing and GIS, prediction of future LULC and analysis of change detection. In this section, an overview of LULC change aspect of global environmental change, earlier scientific investigations on the study of LULC and Future prediction of LULC with various tools and techniques will be presented.

Some of the previous research works related to LULC change and LULC prediction using CA Markov model are discussed below:

Ichii *et al.* (2002) analysed the global relationship between NDVI and climatic variables using satellite data and climate records. The results highlighted significant correlations between NDVI and temperature variations in the northern latitudes, as well as correlations involving NDVI, temperature, and precipitation in semiarid regions. The observed trends in NDVI were influenced by temperature rise in the northern latitudes and precipitation decrease in the southern semiarid regions. However, the reasons behind NDVI increases in equatorial regions require further investigation and could be influenced by multiple factors such as forest regrowth, deforestation, and fertilization.

Chen *et al*. (2004) aimed at iteratively align the data with the upper range of NDVI values and record changes in NDVI patterns. We have seen encouraging outcomes when we applied this newly developed technique to a 10-day Maximum Value Composite (MVC) SPOT VGT-S product. Along with setting the new method's optimal parameters, we evaluated how well it performed in comparison to the BISE algorithm and Fourier-based fitting techniques. According to the results, our novel technique is better at producing NDVI time-series of high quality. As a conclusion, we have solved the problem of residual noise in NDVI time-series data by providing a straightforward yet efficient method based on the Savitzky Golay filter. With the help of this technique, the influence of atmospheric variability and cloud contamination on the NDVI signal is successfully reduced, resulting in better data quality. Findings showed how effective this method is in comparison to other approaches, giving researchers a useful tool for precisely analysing NDVI time-series data.

Jiang *et al.* (2006) conducted a study to investigate the relationship between fractional vegetation cover and the Normalised Difference Vegetation Index (NDVI) and how it varies with spatial scale. Findings showed strong NDVI-on-spatial-scale dependence over a variety of surfaces, suggesting that NDVI values at various resolutions may not be directly comparable. Over partially vegetated areas, particularly where there are darker soil backdrops or shadows present, the NDVI nonlinearity becomes more prominent. Due to its nonlinearity and the impact of scale, utilising NDVI alone may not be appropriate for reliably measuring the vegetation proportion. The Scaled Difference Vegetation Index (SDVI), a scale-invariant index based on linear spectral mixing of red and near-infrared reflectance's, was suggested as a more suitable and reliable method for vegetation fraction retrieval using remote sensing data, especially over heterogeneous surfaces. Although a study used experimental field data to confirm the suggested strategy, additional satellite-level validation would be required.

Behera *et al*. (2012) conducted a study on the impact of unfavorable land use and land cover practices (LULC) on the state of watersheds. This involved examining the consequences of activities such as deforestation, expansion of agriculture, and the development of infrastructure. In order to examine LULC dynamics and forecast possible future events in the Choudwar watershed in India, remote sensing and GIS techniques were combined with the Cellular Automata (CA)-Markov model. The study identified biophysical and socioeconomic variables that influenced the regional pattern of LULC by looking at satellite-derived maps from the years 1972, 1990, 1999, and 2005. While woods, wetlands, and marshy terrain receded, agricultural and populated areas saw tremendous linear development. The study evaluated annual rates of growth in agriculture and settlement and found that proximity to transportation networks and residential/industrial expansion. For successful watershed management, the forecasted LULC scenario for 2014 provided insightful information. To stop further forest loss and LULC shifts, especially in the lower slopes, the study emphasises the need for improved agricultural practices and more energy subsidies. It highlights the significance of taking long-term trends into account and promotes sustainable practices to safeguard forests and other natural resources.

Gandhi *et al.* (2015) used the Normalised Difference Vegetation Index (NDVI) to provide an improved approach for Change Detection in satellite imagery. In order to classify different types of land cover, including vegetation, water bodies, open spaces, scrub areas, hilly areas, agricultural areas, heavy forests, and thin forests, NDVI uses data from multi-spectral remote sensing. To detect vegetation, the NDVI values are calculated at several thresholds (0.1, 0.15, 0.2, 0.25, 0.3, 0.35, 0.4 and 0.5). For multi-source classification, NDVI and DEM data layers are combined with Landsat TM pictures. NDVI differencing is the method used for Change Detection. The simulation findings showed how well NDVI detects surface features, offering useful information for policymakers' decision-making. Natural disaster forecasting, relief delivery, damage assessment, and the creation of safety measures can all benefit from vegetation analysis. Empirical studies showed that between 2001 and 2006, the amount of forest or shrub land decreased by around 6%, and the amount of barren area increased by about 23%. In contrast, there has been a roughly 19%, 4%, and 7% rise in agricultural land, populated regions, and aquatic areas, respectively. Estimates are also made for the areas affected by curvature, plan curvature, profile curvature, and wetness index.

Halmy *et al*. (2015) examined land use/land cover (LULC) changes in a portion of the northwestern desert of Egypt and used the Markov-CA integrated approach for future predictions. LULC maps were created for 1988, 1999, and 2011 using Landsat Thematic Mapper 5 data and random forests classification. The approach achieved over 90% overall accuracy. Analysis of LULC classes showed three stages of modification dominated by different land uses. The Markov-CA approach successfully predicted LULC distribution in 2011 and projected changes for 2023 based on current trends. The projected scenario indicated increased urbanization, expansion of croplands, growth in quarries, and development of residential centers. These findings can guide wildlife protection and management efforts in the area and serve as a reference for similar studies in arid regions experiencing comparable land use changes.

Roy *et al.* (2015) utilised multi-temporal Landsat images to analyse and forecast land use/land cover (LULC) categories with an emphasis on Bangladesh's southeast hill tracts. Seven LULC categories were produced by combining supervised classification methods with NDVI data. Overall accuracy assessments for all three years revealed over 90% accuracy. From 1989 to 2014, the categories of hilly forest, shrub land, and crop land underwent considerable modifications, according to change analysis. LULC for 2014 was predicted using Markov chain-cellular automata modelling, and LULC for 2028 and 2042 was simulated. High accuracy was shown in the validation of the observed and forecasted LULC maps. According to the simulation results, shrub land, crop land, and settlement areas increased while hilly forest and water reservoirs decreased. Insightful management and policy decisions relating to biodiversity, forests, land, and natural resources in the study region are made possible by these findings.

Singh *et al.* (2015) used remote sensing and GIS methods to track changes in land use/land cover (LULC) in the heavily populated Allahabad district of India. The Cellular Automata (CA)-Markov Chain Model (CAMCM) is used to detect changes in LULC that are both spatially and temporally distributed. Validation was carried out using a ground-based land cover image from 2010, while calibration and optimization of the model were carried out using photos from 1990 and 2000. The model was then employed to forecast 2020's likely LULC changes. The investigation showed that socio-economic and biophysical factors had a substantial impact on the development of agricultural areas and settlements in the region. The Land Consumption Ratio (LCR) and Land Absorption Coefficient (LAC), two urbanization indices, showed significant changes in urbanization. The anticipated LULC scenario for 2020 gives LULC planners and policymakers helpful insights to efficiently manage the district and create land use rules. Additionally, recommendations for developing policies are given to guarantee the preservation of this significant land resource.

Mondal *et al*. (2016) examined the validity of the Cellular Automata (CA) Markov process for forecasting future changes in land use and land cover (LULC) and conducted a statistical independence test. Various statistical criteria, including the Kappa Index of Agreement (KIA) and its related variations, were used to validate the CA Markov process. To determine whether the Markov chain approach was appropriate, the statistical test of independence (K2) was used, and the goodness-of-fit hypothesis (Xc2) was investigated. The findings suggested that the statistical independence hypothesis was not supported and that the trends in changing land use and cover were consistent with earlier patterns of development. The actual transition probability matrix did, however, correlate well with the anticipated transition probability generated from the Markov chain approach, as evidenced by the acceptance of the goodness-of-fit hypothesis (Xc2). Kno = 0.8347, K location = 0.859, K location Strata = 0.8591, and K standard = 0.7928 were the statistical values attained.

Mukhopadhaya (2016) focused on simulating changes in land usage in the Doon Valley. The projection of future developments up to 2020 was based on two distinct time periods, 2006 and 2013. To model land use change, the study used Markov Chain Analysis and Cellular Automata Analysis. To show the changes in land usage from 2006 to 2013, a transition probability matrix was developed. A contiguity filter was used to simulate the development of land usage from 2013 to 2020 using CA Markov. By comparing the predicted 2013 Land Use Land Cover (LULC) map with the actual 2013 LULC map, the model's validity was evaluated, and the comparison produced a comparable result with an overall error of 0.019%. Overall increases in agricultural land, fallow land, and vacant land were shown to be 124.42%, 0.77%, and 3.77%, respectively, on the final forecasted 2020 LULC map. On the other hand, a predicted decline of 15.20% and a 17.32% decrease in water bodies and forest land, respectively. The development of prediction maps and data analysis were made easier by the CA Markov procedure.

Habib *et al.* (2017) aimed to use NDWI and unsupervised classification approaches to find a reliable and accurate machine learning solution for water body detection. The Dhaka Metropolitan (DMP) region was selected as the case study area. The investigation used low and mid resolution Landsat sensor data from 1975, 1995, and 2014.The study's key findings showed a purposeful decline in the water bodies of the DMP region, with a reduction rate of 14.83 percent between 1977 and 2014. Another important discovery showed that, for both area and accuracy assessment, the NDWI method beat unsupervised classification strategies. The NDWI method had an accuracy of 86% compared to the unsupervised classification strategies' 66%. Based on these findings, the study draws the conclusion that for the identification of water bodies, the NDWI method is more dependable and accurate than unsupervised classification techniques. The study advises using NDWI methods for precise water body recognition.

Mekonnen and Ghosh (2017) Employed Landsat 5 and 7 Thematic Mapper (TM) datasets encompassing the years 1984 to 2014, a period of 30 years. The maximum likelihood technique was used to identify various land use and land cover categories within a GIS environment. The research area was divided into five distinct land use and land cover categories, including urban, agricultural, shrub and bush, desert, and hilly. In the last three decades, the urban area has grown by 31,73 %, or 42.66 square kilometers, according to the findings. The agricultural area, on the other hand, has decreased by 24.53%, or 32.98 square kilometers. During this time period, the average rate of population growth in the region has been 5%. Based on an analysis of the relationship between population growth and urban expansion, it is anticipated that by 2030, the entire region will have been transformed into an urban area. These results highlight the urgent need for effective urban planning and management strategies to guarantee sustainable land use practices and mitigate potential negative effects on urban ecology. Regular monitoring and updating of urban information using geospatial techniques can help decision-makers formulate policies that strike a balance between urban development and environmental protection. By understanding the patterns of land use change, stakeholders can proactively resolve the challenges associated with rapid urbanization and work toward achieving sustainable urban land use in Adama, Ethiopia.

Hamad *et al.* (2018) studied the dynamics of land use and land cover (LULC) in the Halgurd-Sakran Core Zone (HSCZ) of the National Park in Iraq's Kurdistan. To analyse and forecast LULC categories, they used multi-temporal Landsat photos from Landsat 5 TM (1993, 1998, 2003, and 2008) and Landsat 8 OLI (2017). Two business-as-usual (BAU) scenarios are taken into consideration: one assumes that prior trends under UN sanctions (1993–1998–2003) would continue, and the other assumes that trends following the sanctions (2003–2008–2017) will continue. To simulate future land use changes up to 2023, a Cellular Automata-Markov chain model is used. Random Forest is used to categorise LULC classes, and its accuracy is assessed. The second scenario's results shown a trend towards stable and homogeneous zones, which is advantageous for the park.

Liping *et al.* (2018) used research on changes in land usage and land cover to solve issues including landslides, erosion, land planning, and global change. The study's objective is to anticipate the geographical patterns of land use in 2025 and 2036 based on the dynamic changes in land use patterns now observed. To this end, the CA-Markov model is used in conjunction with remote sensing and geographic information system approaches. The study creates land use classification maps for each year using Landsat 5 TM pictures from 1992, 2003, and 2014 as well as Landsat 8 OLI data. Using a Kappa index, the predicted map's accuracy is checked against the actual land use figures from 2014, yielding a result of 0.8128. Jiangle County's expected land use trends for 2025 and 2036 are determined by the study.

Aliani *et al*. (2019) directed on observing and researching land use changes in Talesh County, especially in urban areas. The greatest likelihood technique was used to classify satellite images from the years 2000, 2007, and 2014. The evaluation of the land use maps' accuracy revealed good kappa coefficients and overall accuracy. The land use map for 2028, which was predicted using the CA-Markov model, shows a considerable growth in urban areas and a decline in agricultural land, woods, and wastelands. The model predicts that Hashtpar's surrounding area, notably on its western and eastern boundaries, will see the majority of future development.

Saah *et al*. (2019) used cooperative system design to identify and address the main land cover mapping gaps and challenges experienced in the Lower Mekong (LMR) and Hindu Kush-Himalaya (HKH) region. They concluded that the stakeholder-based strategy has the potential to be utilized in different situations to promote cooperative work towards tackling LULC change issues and developing international networks and collaborations. They also concluded that the development process will be aided by actively involving regional end user groups in dialogue, consultation, and capacity building for fostering greater regional cooperation in land management.

Fariz and Nurhidayati (2020) utilised machine learning in GEE to map the LULC change in the Kapuas watershed. They used Landsat 8 satellite imagery of 2019 and classified LULC into built-up area, vegetation, water bodies, and non-vegetated (barren land). The study concluded that bands 1 to 7 were found to be good combination and yielded highest accuracy.

Liu *et al*. (2020) employed the random forest technique based on the Google Earth Engine (GEE) platform and extensive time stacking of multi-temporal Landsat photos for LULC change analysis in the northeastern Tibetan Plateau. They found that the random forest technique based on the Google Earth Engine (GEE) platform yielded the accuracy ranging from 89.14% to 91.41% and the kappa values higher than 86.55%. In the study region the grassland and woodland made up the majority of the LULC types, with 50% and 25% of the total area, respectively. It was found that the main forces behind the changes in LULC were elevation and population density along with regional economic development. The results gave a reference for supporting in the establishment of sustainable land management and ecological protection policy decisions and identified the primary driving forces behind LULC changes.

Mohamed and Worku (2020) centered on Addis Abeba and the surrounding region, with the goal of simulating LULC dynamics and creating scenario-based forecasts for managing and planning sustainable urban expansion. The research incorporates modelling methods from the Cellular Automata, Markov chain, and Multi-criteria Analytical Hierarchy Process. The data showed that built-up regions are continuously expanding, which is causing LULC classes to become less important environmentally. In comparison to a Business-as-Usual Scenario (BAUS), quantitative landscape measures shown that an Ecologically Sensitive Scenario (ESS) is more effective at preserving sustainable dynamics in the urban area. With controlled losses of water bodies, forests, and arable land, the ESS modelling technique encourages a more balanced urban system while ensuring a slight expansion of built-up areas. This scenario-based simulation provides alternatives for managing and planning sustainable urban growth, both in the study region and in cities that are similar.

Özelkan (2020) focused on answering the following two outstanding research questions: (i) Which NDWI model produces the best results? and (ii) What impact does employing satellite data with 15 m and 30 m spatial resolutions have on accuracy? The General Directorate of State Hydraulic Works (DSI) conducted in-situ lake area measurements, and the area values from the NDWI models were compared to those measurements to determine accuracy. The results of this study showed that the capacity to differentiate water from other classes when using the near-infrared (NIR) region improves as the lake area rises. In particular, lake expansion effects are more accurately captured by the NDWI (Green, NIR) model. The findings also emphasise the importance of manmade factors like irrigation and daily use in determining fluctuations in lake area, in addition to hydrometeorological factors like precipitation and evaporation. In terms of accuracy, NDWI (Green, NIR), NDWI (Green, SWIR1), and NDWI (Green, SWIR2) were found to be in the order of efficacy, from highest to lowest. Additionally, the usage of data with a spatial resolution of 15 m produced better results than data with a resolution of 30 m.

Regassa *et al.* (2020) focused on the spatiotemporal variability of urban land use and land cover (LULC) changes in Adama City over a period of 37 years. The study utilizes geospatial techniques to examine LULC shifts, forecast long-term urban development, and track population growth for informed decision-making. Satellite data from Landsat 1973, 2000, and 2010 is processed using ArcGIS, Erdas, and Idrisi to generate LULC maps through supervised classification. Cross-tabulation of the maps reveals land-use transfers, changes in built-up areas, and spatial transformations. Markov Chain and CA-Markov techniques are employed to model LULC changes and predict future urban land use. The model's accuracy is assessed using Kappa statistics and other validation techniques. The analysis reveals a significant increase in built-up areas from 2% in 1973 to 23% in 2010, with an estimated growth of approximately 60% over the next 30 years (by 2040).

Aksoy and Kaptan (2021) examined forest and (LULC) changes in Turkey's northern area from 2000 to 2020. Using historical data from the created maps, the CA-Markov hybrid model was used to forecast LULC changes for the years 2030 to 2040. By comparing the 2020 LULC map with the anticipated map, the model's dependability was confirmed, yielding an overall accuracy of 80.90% and a Kappa coefficient of 0.74. The study projected a 3.8% increase in total forest area and water surface area for the period of 2020–2040, as well as a 13.9% decrease in agricultural land and a 5.3% decrease in settlement areas.

Baqa *et al.* (2021) urban sprawl analysis and land use/land cover (LULC) classification were utilised to concentrate on the spatial growth of Karachi, Pakistan. The Google Earth Engine's random forest algorithm and Landsat data were both utilised to categories LULC across a number of years. To examine changes in the urban landscape, six urban classes were determined. Future LULC scenarios were forecast using a CA-Markov model. The study found that built-up regions were expanding unpredictably at the expense of agricultural land. Programmes for reforestation increased the amount of vegetation cover. The expansion of the principal and secondary urban cores was noted by the inquiry. By 2030, there may have been an increase in the total urban built-up area, according to the CA-Markov model. For the study of urban sprawl in a rapidly expanding city, the combined approach of remote sensing, GIS, and urban sprawl matrix was beneficial.

Binh *et al*. (2021) aimed to identify the major LULC classes and to calculate and assess the amount and rate of change for these LULC classes for 30-years, in the Dong Thap Muoi, Vietnam. The study used 128 Landsat photos, topographic maps, land use status maps, cadastral maps, and supplementary data to create the LULC maps. The results indicated that 28.9% of unused land in the total area, and had been replaced by paddy by 45.1%, and became the new leading LULC class. forest area decreased from 14.4% - 5.5%. The built-up area rose from 0.3% to 6.2%. The results of this study may aid in the development of exploitation policies and early formation of a diversified agricultural structure and the promotion of the region's advantages.

Floreano and Moraes (2021) used TerrSet 18.3 software to assess the LULC changes in Rondônia for the last ten years (2009–2019) and forecast prospective changes over the following ten. For image classification, they used machine learning methods, more specifically a Random Forest classifier within the Google Earth Engine cloud-based platform. In addition, by taking into account various transition situations, the Markov-CA deep learning method was employed to forecast future LULC changes. According to the study, Rondônia experienced a considerable decline in wooded areas between 2009 and 2019, totaling to about 15.7%. This shows that there is a worrying tendency of deforestation in the area. According to the study's forecast model, around 30% of Rondônia's remaining forests are anticipated to be cleared for development by 2030.

Haque (2021) examined the dynamics of land use/land cover (LULC) changes in Tanguar Haor, Bangladesh, from 1989 to 2017. The findings indicate that the major

LULC changes in Tanguar Haor involved the transformation of deep-water bodies into shallow water bodies. However, the expansion of shallow water areas alone does not account for the entire scenario, as one-third of these areas were influenced by vegetation or settlements. Agricultural land exhibited the highest increase among vegetation classes, with approximately one-third of all vegetation covers converting into agricultural land over the 28-year period. The study also reveals a shift in the impact buffer of LULC changes from west to east over the observed years. The majority (over 96%) of the local population in the Tanguar Haor area directly depend on haor resources for their livelihood. However, imbalanced LULC changes have posed a threat to important crops and vital natural vegetation in the haor basin. The depletion of haor resources and imbalanced LULC changes can be attributed to factors such as overexploitation driven by population growth, extreme poverty, and inadequate education.

Huang *et al.* (2021) created an overview of the progress that has been made in the acquisition of NDVI, analyses its uses, and covers crucial challenges and considerations related to the use of NDVI. To be more specific, it focuses on three important aspects: ambient impacts, saturation phenomena, and characteristics connected to the sensor. The application of NDVI can be quite successful if the aforementioned considerations are taken into account and understood. This comprehension is especially vital for the UAS user community, since it is the only way to guarantee a responsible and accurate interpretation of NDVI data.

Khwarahm *et al*. (2021) focused on applying the Cellular Automata (CA)-Markov model to predict future land use and land cover (LULC) changes in the Erbil governorate of the Kurdistan region of Iraq. A change detection study was carried out using 1988, 2002, and 2017 Landsat imagery. On the basis of the classified maps from 1988-2002 and 2002-2017, the hybrid model was utilised to produce LULC maps for 2017 and 2050. Validation of the model's correctness revealed good agreement between the model's output and the classified 2017 LULC map. Built-up land, agricultural land, plantations, dense vegetation, and water bodies are expected to grow significantly in the future, while barren land and sparse vegetation are predicted to decline. The study's conclusions have effects on environmental scientists, biologists who specialise in conservation, NGOs, decision-makers, and urban planners.

Prawin *et al.* (2021) used Sentinel-2B satellite imagery in Tiruppur for classification of LULC. Various algorithms like K-means, Iso-Data, support vector machines (SVMs), and maximum likelihood (ML) classification are used. Following that, training pixels are chosen from the remaining classes to run several supervised learning methods for the first and second-level classification, comparing them in terms of accuracy rates. Overall accuracy and the kappa coefficient were used and accuracy was evaluated using metrics derived from an error matrix. In conclusion, a highly accurate algorithm for mapping metropolitan regions was suggested. Due to the algorithm's very few difficult decision boundaries, the support vector machine (SVM) generated the highest overall accuracy and kappa coefficient. For upcoming research, the data are useful in determining how well the classification method performs.

Rahnama (2021) simulated changes in land use and land cover (LULC) in the Mashhad metropolitan region using Sentinel-2A satellite imagery and the Cellular Automata (CA) Markov chain model. Using maximum likelihood estimation, the KAPPA coefficient, and the ROC curve, LULC is divided into seven groups. In 2016, there were 177 rural villages within the 105,243.6-hectare research area. Between 2016 and 2020, there were 7,845 hectares of LULC changes, mostly an increase in built-up areas by 436.32 hectares (5.56%) and a decrease in barren lands by 7,174 hectares (91.45%). Mass and light vegetation showed the greatest decline in land usage, with 1,335 hectares (17.01%) and 5,241 hectares (66.81%), respectively. Using the CA Markov chain model, forecasts for the years 2020–2030 indicate a 2,626.2 hectare change in land use. Negative changes are forecast for light vegetation (-5.70%), dense vegetation (-23.35%), roads (0.34%), and water level (-23.40%), while positive changes are anticipated for barren lands (5.5%), constructed lands (13.5%), and mountainous lands (2.32%). The KAPPA coefficient (0.58) and the area under the ROC curve (0.61) were used to evaluate the classifications' accuracy. In the north and east of the city, a spatial-temporal transition from agricultural and vegetated areas to bare ground and built-up areas is anticipated.

Subedi and Dev Acharya (2021) aimed to evaluate how well the Normalised Difference Water Index (NDWI) did at locating the smallest bodies of water in three districts in western Nepal's south. In addition, we looked at how the water system had changed in the same area during the previous 20 years. In order to do this, we applied thresholds of 0.25 and 0.5 to Landsat scenes from 2002 and 2021. We compared the findings with the pond survey database kept by the Government of Nepal in order to confirm the accuracy of NDWI. The results showed that while NDWI was excellent at spotting the shrinking of bigger water bodies, it was less good at spotting smaller water bodies like man-made ponds. The smallest water bodies found have an extent between 0.44 and 1.03 hectares. Based on our findings, we advise routine water body monitoring in order to precisely measure changes and foresee long-term effects. We also recommend that appropriate authorities make use of high-resolution satellite or unmanned aerial vehicle (UAV) photography to enhance the precision of water body mapping and lessen the requirement for significant fieldwork.

Tadese *et al.* (2021) intended to evaluate changes in land use and land cover from 1987 to 2017, forecast trends from 2032 to 2047, a total of 240 households provided the information. Forestland, farming, grassland, settlement, and waterbody were the five-land use/land cover classifications found by the study. Farmland and settlement grew from 1987 to 2017 by 17.4% and 3.4%, respectively, whereas grassland and forests shrank by 77.8% and 1.4%, respectively. According to the results, farming and settlement would grow by 26.3% and 6.4%, respectively, from 2032 to 2047, whereas forestland and grassland would decline by 66.5% and 0.8%, respectively. Agriculture expansion, population growth, shifting cultivation, fuel wood extraction, and fire danger were shown to be the primary drivers of land use/land cover change. These results indicate important shifts in land use and land cover that will persist in the future. In order to preserve the Majang Forest Biosphere Reserves' resources, a land use plan should be presented. Additionally, in order to stop additional land conversion, local residents' livelihoods need to be improved.

Thapa and Bahuguna (2021) used supervised classification, change detection techniques, and other methods to track spatio-temporal variance in LULC change between 1989 and 2020 in the Pachhua Dun-Dehradun District, Uttarakhand, India. the overall accuracy and Kappa Coefficient (K) were used. The findings of the change detection analysis show that built-up areas (+247.75%) (110 km^2) had the highest growth rate, with an annual rate of change of 3.55 km^2, or 7.99%, the highest among all

LULC classes during the course of the entire research period of 31 years. It was discovered that 69.9 km^2 of the area under agricultural land had been transformed into built-up areas. In addition, 36.3 km^2 of open, saline ground and 38.9 km^2 of vegetation/forest cover have been turned into agricultural land.

Ahmad *et al.* (2022) investigated the effects that rapid urbanization has had on Lahore, Pakistan's air quality as well as land use and land cover (LULC). Used data from Landsat, GIOVANNI, SRTM DEM, and vectors to perform four essential steps: LULC categorization, future prediction, assessment of air quality consequences, and monitoring. The research indicates that between the years 2000 and 2020, there will be more urban areas and less regions of flora, barren ground, and water bodies. According to projections, urbanization will continue to spread by the year 2040, leading to a concurrent decrease in the amount of vegetation, dry land, and water bodies. Pollutants in the atmosphere including NO_2, SO_2, CO_2, CO, O_3, and CH_4 have all increased, and it is anticipated that this trend will continue until 2040. The majority of urban sprawl development in the city took place in the city's eastern and southern districts. The research highlights the significance of preserving natural resources, particularly plant cover, as a means of reducing air pollution and mitigating the effects of LULC change.

Ambarwulan *et al*. (2022) intended to use remote sensing and Geographic Information Technology to create the LULC map and track changes to it. Google Earth is used to interpret multi-year Landsat imagery for mapping using machine learning and the Random Forest (RF) classifier. Engine (GEE) (GEE). The results showed that built-up land and paddy fields, which increased and reduced by 244% and 69% respectively, were the two primary classifications that saw significant changes in JATABEK. Moreover, RF and GEE are particularly durable in challenging domains like JATABEK. The overall accuracy and Kappa coefficient above 80% serve as evidence for this. To create flood management plans, planners and managers looked at LULC as a whole in JATABEK.

Loukika *et al.* (2022) studied the combined effects of land use and land cover (LULC) and climate change (CC) on water resources in the Indian Munneru river basin. Water availability is evaluated using the SWAT (Soil and Water Assessment Tool) model. The model has been calibrated and tested, and the differences between observed and simulated streamflow are highly correlated. The CA-Markov model predicts changes in LULC, showing an increase in built-up and kharif crop areas and a decrease in barren fields. Three future time periods are examined under various hypotheses for climate change. When both CC and LULC are taken into account, an increase in stream flows is anticipated. In the following periods, the average monthly mean streamflow will increase by a percentage ranging from 33.9% to 45.3% (RCP 4.5) and from 33.8% to 38.8% (RCP 8.5). Aquifer recharge declines as elements of the water balance like surface runoff and evapotranspiration grow. The conclusions offer insightful information for integrated water management strategies taking into account LULC projections and climate change scenarios.

Mathewos *et al*. (2022) aimed to assess the dynamics of LULC in the Matenchose watershed from the years 1991, 2003, and 2020 and future forecast of land use changes for 2050. ETM+ for 2003, Landsat TM for 1991 and Landsat-8 OLI were used to classify LULC for 2020, the ERDAS Imagine software, a supervised picture sorting method was used. Using the classified LULC, the anticipated LULC 2050 was calculated. By taking into account the various LULC dynamics drivers, we may develop CA-Markov and land change models. According to the LULC data from 1991, the watershed was primarily covered by grassland (35%), while in 2003 and 2020. According to the expected outcomes, from 2020 to 2050, cultivated land and settlement rose by 6.36 percent and 6.5 percent, respectively, whereas forestland and grassland dropped by 63.7 percent and 22.325 percent, respectively. This study's findings may aid in making wise decisions and strengthening land use regulations for various forms of land management.

Nasiri *et al*. (2022) aimed at understanding the potential impact of two composition techniques and spectral-temporal metrics collected from satellite time series on a machine learning classifier's capacity to produce precise LULC maps. developed time series for Tehran Province (Iran) as of 2020 using the Google Earth Engine (GEE) cloud computing platform. Seasonal composites and percentiles metrics, two composition techniques, were utilized to establish four datasets based on topography layers, vegetation indicators, and satellite time series. The results concluded that S-2 exceeded the L-8 spectral-temporal metrics at both the class and overall levels, according to accuracy evaluation results. Also, the composition technique comparison revealed that seasonal composites performed better than percentile metrics in both the S-2 and L-8 time series and that this methodology can be applied to large-scale LULC mapping and can quickly and accurately develop LULC maps based on cloud computing GEE.

Setiawan and Nandini (2022) focused on the effects of changes in land use and land cover (LULC) on flooding in the Sari Watershed on the island of Sumbawa in Indonesia. The transformation of forestland into non-forested land may cause an increase in the volume of surface runoff and the frequency of flooding further downstream. Using LULC maps derived from Landsat imagery, the research analyses the impact that changes in LULC will have on peak discharge between the years 1990 and 2030. While the HEC-HMS model is responsible for determining peak discharge, the ANN-CA Markov model is used for analysing LULC changes and making predictions. The examination of correlation demonstrates that there is a constant association between the change in LULC and the dynamics of peak discharge, particularly the shift from forest covering to non-forest coverage. The findings can contribute to the development of measures for reducing the danger of flooding and for LULC planning in the Sari Watershed.

Srivastava *et al.* (2022) examined the classification results of the Support vector machines, Random forests, Gradient tree boosting, and Classification and Regression Tree algorithms (CART) (SVM). The study region has four LULC classes, is situated at 30.3165° N and 78.0322° E close to the foothills of the Himalayas. Sentinel-2 and LANDSAT-8 images were employed as the satellite imagery for the classification. Urban, water, forest, and agricultural points are represented by points with values of 536, 506, 505, and 540, respectively. They were split into subgroups for training (70%) and evaluation (30%). Metrics obtained from an error matrix were used to measure accuracy. Cohen's kappa calculation technique and confusion were used to quantify accuracy. By using a machine learning method to classify land use and cover, we can calculate the percentage of each landcover type in the research area. For calculating change detection and keeping track of additional changes in any land cover class, there is plenty of room for additional researchers in this field.

Yasin *et al.* (2022) used three Landsat datasets: TM (1991), ETM+ (2005), and OLI-TIRS (2019). In order to appropriately quantify these changes, the study used the Normalised Difference Vegetation Index (NDVI) and the Normalised Difference Building Index (NDBI). While the NDBI study sought to identify densely populated urban areas, the NDVI analysis monitored the degradation of vegetation. The NDVI and NDBI density study findings showed a dramatic decline in vegetated land and a sharp rise in the utilisation of urban and built-up area. The conversion of agricultural and forest areas into low-density developments suggests rapid and extensive growth. The study focused on the environmental changes caused by the regional development corridor's fast urban growth, particularly on its perimeter. The approach offered a dynamic perspective and increased the precision of the evaluation of land use and land cover change by using both NDVI and NDBI as surrogates. The results showed that urban growth quadrupled between 1991 and 2019, with the fastest growth taking place between 1991 and 2005, mostly due to low-density construction. In contrast to a more sustainable tendency of higher-density development, the growth pattern has recently grown more erratic.

Agdas and Yenen (2023) focused on evaluating LULC changes in the Lüleburgaz region between 2001 and 2021. and examined the impact of urban growth on natural areas and assessed how these areas are managed within the context of sustainable development goals. Furthermore, the study evaluates the effects of urbanization on land use changes. The accuracy of the LULC maps was assessed using the general accuracy index and the Kappa index. The land use maps for 2001, 2010, and 2021 exhibited overall accuracy rates of 96.32%, 93.66%, and 95.91%, respectively. The corresponding Kappa values were 0.95, 0.91, and 0.94. These results indicate that rapid urbanization and population growth over the past two decades have led to a 4.82% increase in the built environment and a 4.88% decrease in agricultural land. This finding highlights the upward trend in urban development at the expense of a significant reduction in agricultural areas. The study's findings offer valuable data that can assist authorities in making informed decisions to promote sustainable urban planning and improve environmental conditions.

Ait El Haj *et al.* (2023) analysed 20 years' worth of data and satellite pictures of the Lakhdar-Morocco sub-basin to forecast land use change trends from 2019 to 2039. The CA-MARKOV and LCM models are contrasted. Land use categories included by the photos include water bodies, forests, vegetation, and barren land with urban areas. The images used are Landsat 5-TM and Landsat 8-OLI images from 2000, 2007, 2010, and 2019. The kappa index and confusion matrix are used to evaluate the models' accuracy. The findings showed that, mostly as a result of urbanisation, the forest area will dramatically decline in the years to come. Between 2000 and 2039, it is anticipated that forest areas would shrink by 70%, while bare land and urban areas will grow by roughly 37%. The number of plants and water bodies will largely not change. These results underline the need for fresh approaches to safeguard the Lakhdar sub-basin's forests, vegetation cover, and land sustainability from erosion and deforestation.

Amgoth *et al.* (2023) analysed how numerous dynamic factors, such as environmental, economic, and social impacts, affect changes in LULC in Pakhal Lake. Deep learning algorithms were applied to satellite photos from 2016 to 2022 for the LULC categorization, using Sentinel-2 imagery in Google Earth Engine. The classification of LULC changes was done using the Dynamic World dataset, the satellite photos were categorized by dividing them into six separate LULC categories. A Cellular Automata and Artificial Neural Network (CA-ANN) combination technique was used to predict future LULC alterations. To forecast and examine probable LULC changes anticipated by 2025 and 2028, the Multi-Layer Perception (MLP) QGIS plugin MOLUSCE was used. Indicated by an overall Kappa coefficient value of 0.78 and an accuracy rate of 82%, the assessment of the LULC changes and forecasted maps for 2025 produced promising results. The MLP-ANN method was used to forecast LULC changes for the years 2025 and 2028, and the results showed an expected rise in agricultural areas, urban areas, and arid terrain. The findings of this study are highly valuable in helping to advance the creation of better methods for managing natural resources.

Frimpong *et al.* (2023) investigated the phenomena of deforestation, rapid urbanisation, and the loss of cultivable lands. Landsat satellite images from the years 1986, 2003, 2013, and 2022 were utilised in order to conduct the analysis. The images were utilised to conduct an analysis of Land Use Land Cover (LULC) changes in the Kumasi Metropolitan Assembly and surrounding municipalities. The employed methodology utilised the Support Vector Machine (SVM), a machine learning algorithm, for the purpose of satellite image classification and the subsequent generation of Land Use and Land Cover (LULC) maps. An investigation was conducted to evaluate the correlations between the Normalised Difference Vegetation Index (NDVI) and Normalised Difference Built-up Index (NDBI). Annual deforestation rates were determined by overlaying forest and urban extents. The results of the study revealed a decreasing pattern in forested areas, a rise in urban and built-up regions (which corresponded with the image overlays), and a reduction in agricultural lands. A negative correlation was observed between the Normalised Difference Vegetation Index (NDVI) and Normalised Difference Built-up Index (NDBI). The findings emphasise the critical need for the utilisation of satellite sensors in conducting a comprehensive assessment of land use and land cover (LULC).

Gaur and Singh (2023) analysed methods and strategies used in Land Use Land Cover (LULC) modelling. By providing a summary of the current techniques and modern concepts used in LULC modelling. The paper highlights the potential advantages of integrating various approaches, such as machine learning models with statistical models, to improve LULC modelling and take advantage of their individual capabilities. Even though LULC modelling has come a long way, the assessment emphasizes how crucial it is to incorporate policy frameworks into the modelling process in order to support better urban planning and administration. The goal of this study is to assist academics and policymakers in implementing improved land management techniques that are in line with Sustainable Development Goal-15 (SDG-15), which is concerned with maintaining life on land.

Ghasempour *et al*. (2023) sought to compare the Landsat 8 and 9 LST results using ground-based data obtained from the Surface Radiation Budget Network and examine the performance of Landsat 8 and 9's multispectral bands in LULC mapping by employing the Random Forest (RF) method (SURFRAD). The Google Earth Engine (GEE) environment was used to execute RF-based categorization and pixel-based LST information extraction. Using the LULC categorization, the IDR province of Turkey was chosen as the study area. LULC mapping was done using Collection 2 Level 2 Surface Reflectance (SR) Products from Landsat 8 and Landsat 9. On the other hand, LST analysis was done using the Collection 2 Level 2 Surface Temperature (ST) products. According to the LULC data, Landsat 9 performed better in this case study than Landsat 8, with Kappa values and Overall Accuracy (OA) of 87.4%, 0.83, and 82%, 0.76, respectively. A study demonstrated that OLI and TIRS sensors on Landsat 9 are superior to those on Landsat 8.

Maruf *et al.* (2023) aimed to assess the valuation of ecosystem services (ESV) in Cox's Bazar district, considering its significance as a tourist destination and the significant land use and land cover (LULC) changes it has experienced. The study focuses on understanding the impact of LULC changes on crucial natural resources such as forests, wetlands, and beaches, which have been affected by tourist pressure and the migration of Rohingyas. By assessing different land-use scenarios, the study aims to determine the effects on ESVs and their implications for sustainable development. Satellite images from LANDSAT spanning 20 years were used, and ESVs were calculated for different intervals. The findings highlight the LULC classes most prone to ESV changes and provide insights into how ESVs evolve over time. The results of this study can contribute to sustainable land management policies and the preservation of forests, beaches, and wetlands by controlling encroachment.

Sujarwo *et al.* (2023) studied Mayang Watershed, which covers a total area of 1,110.14 km^2, and analysed using Landsat photos from 1970 all the way through 2020. Images acquired from the Landsat 1 MSS, Landsat 5 TM, Landsat 7 ETM+, and Landsat 8 OLI/TIRS satellites and processed using open-source software were utilised in the research project. The LULC maps for the years 1972, 1997, 2002, 2017, and 2020 were constructed using a Gaussian maximum likelihood classifier. An analysis showed that there was a moderate increase in pavement areas between the years 1972 and 1997, followed by an exponential growth between 1997 and 2020 at a rate of 7.5% each year. This rapid expansion is evidence of changes caused by humans, which are having an effect on paddy fields and limiting the amount of diverse agricultural land.

Tariq and Mumtaz (2023) used remote sensing data to anticipate changes in land use and land cover (LULC) using cellular automata (CA) and Markov chain models. Using data from Landsat TM, ETM+, and OLI/TIRS, LULC distributions were mapped for the years 1990, 2006, and 2022. The long-term landscape changes from 2022 to 2054 at 16-year intervals were simulated using a CA-Markov chain. Support vector machine (SVM) was also used in the analysis to examine urban sprawl. According to the data, based on observed changes from 1990 to 2022, the built-up area will grow from 285.68 km^2 (22.59%) to 383.54 km^2 (30.34%) between 2022 and 2054. Addressing these trends is essential if we are to stop deforestation and achieve sustainable development. This study helps local government agencies plan for the future while preserving natural resources by offering insightful information for land cover management techniques.

The literature review pertaining to Land Use and Land Cover (LULC), LULC prediction, and LULC analysis offers significant insights into the constantly changing state of our environment and the growing necessity for precise and effective monitoring and administration of land resources. Through analysis of the existing literature, scholars and professionals can expand upon prior discoveries and devise novel methodologies to tackle present and forthcoming obstacles in the domains of land use planning, ecological preservation and sustainable growth. The literature review presented here serves as a fundamental basis for future research endeavors. This highlights the importance of interdisciplinary collaboration to advance our understanding of land use and land cover (LULC) dynamics. This facilitates informed decision-making for the benefit of current and future generations.

Materials and Methods

Chapter 3 MATERIALS AND METHODS

This chapter deals with the description of the study area and data acquisition. The methodology comprises of the extraction of LULC map using landsat satellite, analyzing the changes in LULC and methods used in prediction of future LULC using TerrSet (version 19.0.5).

3.1 Study Area

The Doddahalla watershed is situated in the Chitradurga district of the Indian state of Karnataka and is a part of the lower Tungabhadra catchment of the river Krishna. The watershed spans an area of around 1082 km^2 and covers the taluks of Hiriyur, Challakere, and Chitradurga (Fig. 3.1).

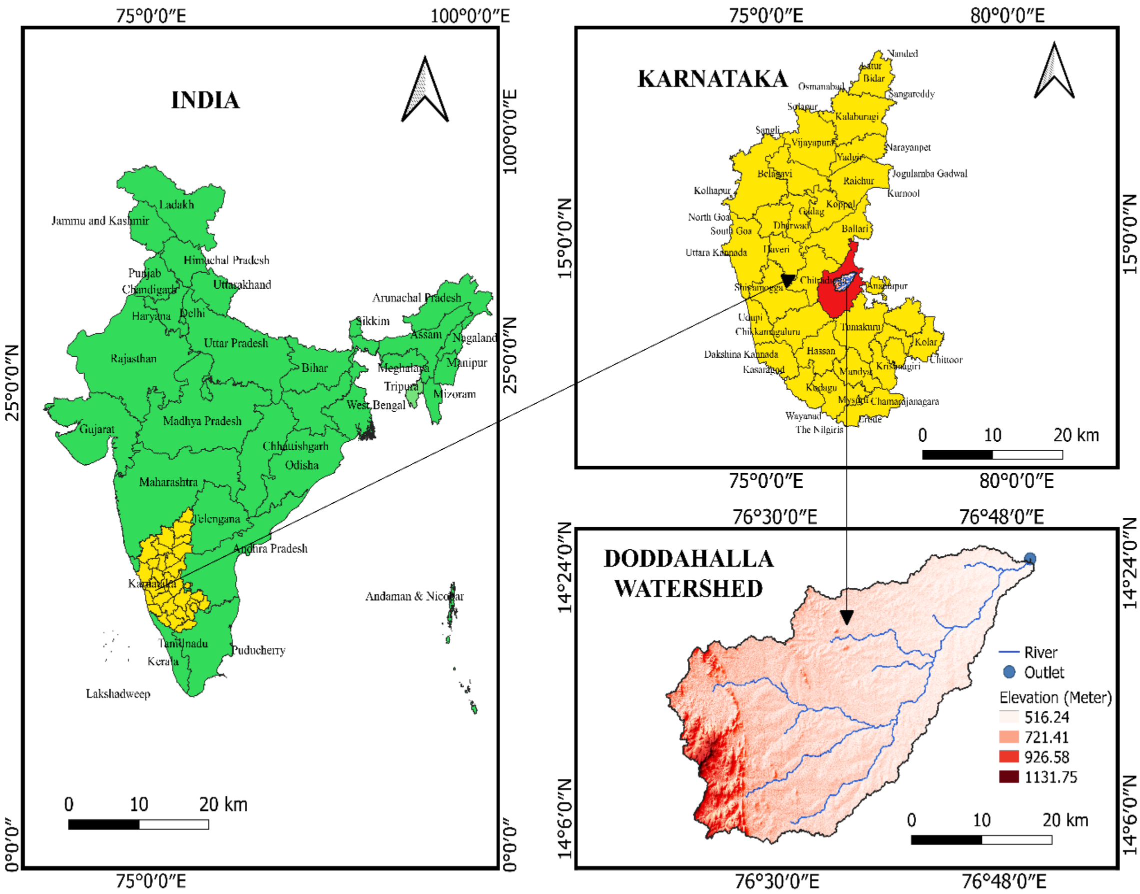

Fig. 3.1: Location map of the study area

Its geographical coordinates ranges from 76°21′10″ East to 76°50′30″ East longitude and 14°4′9.42″ North to 14°25′00″ North latitude. The Doddahalla River originates at an elevation of approximately 780 meters and joins the Tungabhadra River at an elevation of about 510 meters. The topography of the region is characterized by undulating hills, linear ridges, plains, and other features. The predominant types of soil in the area are black, red, and red loamy soils. The watershed can be described as parched and arid, with shattered hill ranges and undulating plains. The region experiences a semi-arid climate and receives an average annual precipitation of 578 millimeters, with the southwest monsoon accounting for 50% of the total precipitation. Agriculture is the primary occupation in the district, with 78% of the land being used for agricultural purposes. The success of agricultural seasons depends on rainfall and the use of tanks. Kharif season, which occupies 60% of the net crop land, is entirely dependent on rainfall. Double cropping is only feasible along the abandoned water sources, such as tanks and streams. The forests in the region are home to a variety of vegetation, including native vegetation.

3.2 Data Collection and pre-processing

The Required data was collected from USGS earth explorer (www.earthexplorer.usgs.gov) and processed using Arc GIS 10.4.1 software. This data is easily accessible to users for a wide range of applications, such as monitoring and classification of land use and land cover changes. The Landsat satellites, including Landsat-7, Landsat-8 (Fig. 3.1), and the newly launched Landsat-9, provided the most popular data sets available. The different RS images provides deeper understanding of the environment, including vegetation health, water supplies, and land use patterns, by utilizing the distinct spectral properties of each Landsat band. Additionally, I collected various data as a model's drivers for prediction of future LULC using TerrSet software (version19.0.5). In our classification approach I’m using versions of landsat (landsat-7 and landsat-8) data sets.

Data collection was a crucial step in the watershed delineation process, as it formed the foundation for subsequent analyses. Data collection for watershed delineation typically involved gathering information on the terrain, land use *etc*. of the study area. SRTM (Shuttle Radar Topography Mission) data was used to delineate the watershed. Once the data points were obtained, they are processed to create a raster image, where each pixel represented a specific elevation value.

3.2.1 Remote sensing data for LULC assessment

Table 3.1. Descriptive Table of Landsat-7 and 8 Satellite Characteristics

Landsat-7 data	• Landsat 7 is a satellite launched on April 15, 1999, by NASA and is part of the Landsat program. • The satellite orbits the Earth at an altitude of 705 kilometers and has a polar orbit. • The Landsat 7 satellite is equipped with a sensor called the Enhanced Thematic Mapper Plus (ETM+), which captures images of the Earth's surface in seven spectral bands, including visible, near-infrared, and thermal. • The satellite can capture images of the Earth's surface with a spatial resolution of 15 meters for most of the spectral bands and 60 meters for the thermal band. • The Landsat 7 satellite provides global coverage of the Earth's surface every 16 days.
Landsat-8 data	• Landsat 8 is the latest satellite in the Landsat program, launched by NASA on February 11, 2013. • Landsat 8 captures images with a spatial resolution of 30 meters per pixel, which provides a high level of detail in the imagery. • Landsat 8 also has a Thermal Infrared Sensor (TIRS) instrument that captures images in two thermal bands.

The process of data extraction from Landsat satellite images involves several steps, as outlined below:

a) **Acquisition of Landsat Images:** The first step was to acquire Landsat images from USGS Earth Explorer website. These images were usually in a digital format and could be downloaded for free. Details of various bands of Landsat 7 and 8, their resolution and wavelength ranges are expressed in Table 3.3 and Table 3.4 respectively.

b) **Pre-processing:** The raw Landsat images contain noise and other artifacts that can affect the accuracy of the data extraction process. Therefore, pre-processing was done to correct these issues. This includes atmospheric correction, as well as geometric correction to remove distortions caused by the satellite's orbit.

c) **Image enhancement:** Image enhancement techniques are used to improve the quality of the Landsat images and to highlight specific features of interest. This could include contrast stretching, histogram equalization, and edge detection.

d) **Classification:** Once the Landsat images were pre-processed and enhanced, they could classified into different land cover types using remote sensing algorithms. These algorithms use the spectral characteristics of the image to differentiate between different types of land cover, such as forests, urban areas, and water bodies.

e) **Validation:** The accuracy of the data extraction process was validated to ensure that the results were reliable. This can be done by comparing the classified image with ground truth data, such as data collected from aerial photography.

3.3 Image Classification

The identification and mapping of land cover classes was achieved through the utilisation of digital remotely sensed data, employing a technique referred to as supervised digital image classification. The primary objective of this methodology was to assign land cover classifications or themes to each individual pixel within an image in an automated manner. The maximum likelihood classifier. a commonly employed classification method in the field of remote sensing due to its capacity to quantitatively evaluate the variance and covariance of spectral response patterns across diverse land cover categories. The classifier under consideration was based on statistical parameters and was widely recognised as one of the most precise techniques. The supervised classification was conducted utilising digital topographic maps and ground checkpoints of the study area. To improve the precision of land cover classification for the two images, the supplementary data sources and the findings of visual interpretation with the classification output through the use of GIS (Geographic Information System). The objective of this integration was to enhance the overall precision of the classified image by integrating additional data.

3.3.1 Maximum Likelihood Classification

The Maximum Likelihood Classification (MLC) technique is a prevalent and extensively employed approach in the classification of remote sensing images. The process involves the utilization of a statistical algorithm to allocate pixels within an image to distinct land cover categories, predicated on their spectral characteristics. The Maximum Likelihood Classification (MLC) method is found on the principle of maximum likelihood estimation. This method presupposes that the probability distribution of pixel values for each class in the image is specific. The Maximum Likelihood Classification (MLC) algorithm was employed to estimate the probability of a given pixel being associated with a specific class. This was accomplished by contrasting the spectral signature of the pixel in question with the spectral signatures of established training samples. The training samples were carefully selected to exclusively represent the pure pixels of each land cover class that was of interest. In the course of classification, the algorithm evaluated the likelihood of a pixel being assigned to a specific class by computing the spectral resemblance between the pixel and the training samples. The pixel was assigned to the class with the highest probability. The utilization of the Maximum Likelihood Classification (MLC) technique involved the consideration of the statistical distribution of the pixel values within each class. This approach enabled improved discrimination between classes those exhibit overlapping spectral signatures. The multi-layer perceptron classifier exhibited proficiency in processing multi-dimensional data by taking into account not only the spectral bands but also supplementary information, such as texture or contextual features. The estimation of posterior probability for each pixel's class membership was a valuable feature offered by MLC, as it allowed for the quantification of uncertainty.

Table 3.2 Details of the LULC Data Set for each decade.

Data set	Data Source	Spatial resolution	Data format
LULC 2003	Landsat 7 ETM+	30m	Landsat 7 ETM+ Collection 2 Tier 1 TOA Reflectance
LULC 2013	Landsat 8 OLI	30m	Landsat 8 Collection 2 Tier 1 TOA Reflectance
LULC 2023	Landsat 8 OLI	30m	Landsat 8 Collection 2 Tier 1 TOA Reflectance

Table 3.3 Landsat 7 band classification

Band Number	Resolution (m)	Wavelength Range (µm)
1	30	0.45 - 0.52
2	30	0.52 - 0.60
3	30	0.63 - 0.69
4	30	0.77 - 0.90
5	30	1.55 - 1.75
6	30	2.08 - 2.35
7	30	2.09 - 2.35
8	30	0.52 - 0.90
9	30	1.36 - 1.39

Table 3.4 Landsat 8 band classification

Band Number	Resolution (m)	Wavelength Range (µm)
1	30	0.435 - 0.451
2	30	0.452 - 0.512
3	30	0.533 - 0.590
4	30	0.636 - 0.673
5	30	0.851 - 0.879
6	30	1.566 - 1.651
7	30	2.107 - 2.294
8	15	0.503 - 0.676
9	30	1.363 - 1.384
10	30	10.60 - 11.19
11	30	11.50 - 12.51

(Source-https://www.usgs.gov/landsat-missions/landsat-7)

3.4 Accuracy Assessment

Accuracy assessment is an essential step in the process of creating land use and land cover (LULC) maps. The purpose of accuracy assessment is to evaluate the quality of the classification and determine how well the map represents the real-world land cover conditions. Accuracy assessment was typically conducted by comparing the classified LULC map to a reference dataset, such as high-resolution aerial or satellite imagery, ground truth data, or existing maps. The reference dataset was used as a benchmark to measure the accuracy of the classification. There are several measures used to assess the accuracy of LULC maps, including overall accuracy, producer's accuracy, user's accuracy, and Kappa coefficient. These measures are described as follows:

3.4.1 Overall accuracy

This is the proportion of correctly classified pixels in the LULC map. It is calculated as the ratio of the number of correctly classified pixels to the total number of pixels in the map. The overall accuracy for Land Use/Land Cover (LULC) classification is calculated using the error matrix generated by the classifier. The error matrix is a table that compares the classified results with the reference data (ground truth) and shows the number of correctly classified and misclassified pixels for each class.

The formula for overall accuracy is:

$$Overall\,Accuracy = \frac{\left(\sum diagonal\ elements\ of\ error\,matrix\right)}{\left(\sum all\ elements\ of\ error\,matrix\right)} \qquad \dots (3.1)$$

where the diagonal elements represent the number of correctly classified pixels and the sum of all elements represents the total number of pixels in the image.

3.4.2 Producer's accuracy

This measures the accuracy of a specific land cover class in the LULC map. It is calculated as the ratio of the number of correctly classified pixels in a particular class to the total number of pixels in that class in the reference dataset.

It is calculated using the following formula:

$$Pr\,oducer's\,Accuracy = \frac{\left(Number\,of\ correctly\,classified\ samples\,in\,a\,class\right)}{\left(Total\,number\,of\ samples\,in\,that\,class\right)} \quad . (3.2)$$

The Producer's Accuracy is expressed as a percentage, where a higher value indicates more accurate classification result. It is one of the most commonly used metrics for evaluating the performance of a land cover classification algorithm.

3.4.3 Kappa coefficient

The kappa coefficient is a statistical measure of inter-rater agreement or reliability, which is commonly used in research studies where multiple raters or judges are required to rate or classify the same set of items or cases. This measure is particularly useful when dealing with subjective or categorical data, such as the interpretation of medical images or the assessment of the severity of a disease. The kappa coefficient is a number between -1 and +1, where 1 represents perfect agreement between raters and 0 indicates agreement due to chance alone. A negative value of kappa indicates that the agreement between raters is worse than random, and it may occur when the raters are intentionally trying to disagree with each other or when the measurement tool is unreliable.

The formula for the kappa coefficient is:

$$Kappa\ Coefficient = \frac{(TS \times TCS) - \sum(column\ total \times rowtotal)}{(TS)^2 - \sum(column\ total \times rowtotal)} \times 100 \qquad \ldots (3.3)$$

Where,

TS- Total Sample Number

TCS-Total Correct Sample Number

The kappa coefficient has several advantages over other measures of inter-rater agreement, such as the percentage agreement or Cohen's kappa. It takes into account the possibility of agreement due to chance, which is often a concern in studies with low prevalence of a condition or when the categories are highly imbalanced. Moreover, it can handle more than two raters and more than two categories.

3.5 Predicting Land Use and Land Cover Changes with CA-Markov

CA-Markov has emerged as a highly effective strategy for accurately predicting changes in Land Use and Land Cover (LULC), surpassing other approaches in terms of performance **(Potapov *et al.,* 2012)**. Due to its reliability, CA-Markov has gained prominence in the field of LULC prediction. It offers the unique capability to forecast transitions between different LULC classes in both the forward and backward directions, as noted by **Pourghasemi *et al.* (2013)**.

The application of CA-Markov involves a three-step process for predicting future LULC changes. It is important to note that CA-Markov's effectiveness lies in its ability to model and simulate the dynamic nature of LULC changes. It accomplishes this through the following steps:

a) Model Initialization: In this step, the initial LULC conditions and spatial parameters are defined. The existing LULC data is utilized to establish the starting point for the simulation. This involves collecting and processing historical LULC data, land use policies, and any other relevant information required for accurate initialization.

b) Transition Potential Estimation: Once the model is initialized, the transition potential between different LULC classes is estimated. It involves analyzing the relationships and patterns observed in the historical data to determine the likelihood of transitions occurring between various land cover types. Factors such as proximity, accessibility, land suitability, and socio-economic variables are considered to quantify the transition potential.

c) Simulation and Prediction: In the final step, the CA-Markov model simulates the LULC changes over a defined time period based on the estimated transition potentials. It takes into account the initial conditions, transition probabilities, and the spatial dynamics of the study area. The model iteratively predicts the future LULC states by applying the transition potentials to each cell or unit of analysis. This iterative process continues until the desired time period is reached, generating a prediction of the future LULC pattern.

3.5.1 Land change modeler (LCM)

The Land Change Modeler (LCM) is a widely used tool for analyzing and predicting land use change, particularly in assessing its impact on biodiversity. This model is integrated into the TerrSet Software (version 19.0.5) program and enables the generation of initial estimates of changes between two distinct time periods based on categorized maps and acquired categories (e.g., losses, gains, net changes, trends of change). The results of these changes are visualized through graphs and maps, facilitating the development of prospective transition models among different land use categories while considering statistical and dynamic factors. To forecast future land use and land cover (LULC) changes, LCM utilizes either the Multi-Layer Perceptron (MLP) method or logistic regression. In this study, the MLP neural network was employed due to its superior performance in complex and nonlinear systems, and its endorsement by reputable publishers. Consequently, the LCM model utilized the LULC maps to assess and evaluate transformations in various land use categories, as well as generate transition potential maps that contribute to the understanding of future changes affecting the landscape.

3.5.2 Cellular automata approach

Cellular Automata, often known as CA, are discrete dynamic systems that determine the state of every cell at time t+1 based on the circumstances of neighboring cells in accordance with a set of predetermined transition rules. CA is a method for replicating the temporal and spatial motion or evolution of objects in two dimensions. This can be done in either dimension. The CA model takes into account both global and local actions, which makes it possible to simulate global shifts using just local computations. Global models use the assumption that all variables are the same, yet they might not be able to properly capture specific conditions that are localised. The CA approach has been more popular for modelling urban growth as a result of its capacity to describe a complex spatial nature using principles that are both straightforward and efficient. The discrete lattice or physical environment (L), the set of potential states in each cell at time step t (ε), the neighborhood defined as all cells within the radius of the current cell (ℵ), and the local transition rule (δ) are the components that make up the representation of a CA model as a discrete dynamic system. These four components make up the representation of a CA model as a discrete dynamic system. **Ahmed and Ahmed (2012)** assessed these four elements and the formula to be computed in the processes (Equation 3.4).

$$\aleph_s r = \left(\frac{i_1, i_2}{dist(i_1, i_2)} \prec r \right) \qquad \dots (3.4)$$

Where dist $(i_1, i_2) = \left(\sqrt{i_1^2 + i_2^2} \right)$

ℵsr = the relative index of all neighbors of a particular cell (Equation 3.5)

$$\delta : \Sigma^{|\aleph|} \rightarrow \Sigma : U_{j \in \aleph_i(t)} \sigma_i \rightarrow (t+1) \qquad \dots (3.5)$$

The equation illustrates that the condition of the i^th^ cell at the next time step, t+1, is determined by the local transition rule, δ, which considers the conditions of all cells within its neighborhood at the current time, t. In this context, ℵi(t) represents the specific neighborhood associated with the i^{th} cell at time t, while |ℵ| denotes the number of cells encompassed within the neighborhood. The local transition rule is defined by a rule table that defines the sizes of Σ and ℵ, resulting in a total number of possible rules denoted as ΣΣℵ. Each of these possible configurations within a cell's neighborhood, Σℵ, corresponds to a specific set of conditions that the cell can adopt. Thus, when considering the ordered set of all cell conditions collectively at time step t, it represents the global arrangement of the CA.

The Markov chain model was used to generate a transition probability matrix between an initial state and a final state as an input to the CA-Markov model. Transitional probability matrices were created to analyze how each land cover class were predicted to change. The following equation may be used to explain the Markov model:

$$S(t+1) = P_{ij} - S(t) \qquad \dots (3.6)$$

Where,

S represents the land use condition at time t

S (t + 1) represents the land use status at time (t + 1) and P_{ij} is the transition probability matrix in a certain state, which was calculated using the following equations;

$$\|P_{ij}\| = \begin{Vmatrix} P_{1,2} & P_{1,2} & P_{1,N} \\ P_{2,1} & P_{2,2} & P_{2,N} \\ p_{N,1} & P_{N,2} & P_{N,N} \end{Vmatrix}$$

$$\left(0 \leq P_{ij} \leq 1\right) \qquad \ldots (3.7)$$

Where,

P refers to the transition probability

Pij refers to the probability of changing from state i to state j in the next time and

PN refers to the state probability of any time.

The low transition probability is close to 0, and the high transition probabilities is close to 1

$$KIA = \frac{Pr(a) - Pr(e)}{1 - Pr(e)} \qquad \ldots (3.8)$$

where,

Pr(e) denotes chance agreement and Pr(a) denotes the observed agreement.

3.6 Prediction of future LULC dynamics

Future land use change modeling is not confined to a specific category of models, as different studies have been conducted to select the most accurate prediction model. In this study, two approaches, namely the empirical-statistical model (LCM) and the stochastic model (CA-Markov), were utilized to simulate land use changes. Both models shared similarities in their ability to forecast future dynamics using a transition probability matrix. However, their implementation differs in terms of the integration of variables and processes. The methodology employed for simulating these two prediction models is presented in (Fig. 3.3).

3.6.1 Analysis on dynamic change rate of land use

The measurement of land use change rate provides an indication of the extent of land use transformation within the study area during a specific time interval. The evaluation standards consist of two metrics: the single land use dynamic degree (Equation 3.9) and the comprehensive land use dynamic degree(Equation 3.10). In this research, both the single land use dynamic degree and the comprehensive land use dynamic degree were employed to assess the rate of land use change.

The formulas are as follows:

The single land use dynamic degree:

$$S_i = \frac{LA_{(i,t1)} - ULA_i}{LA_{(i,t1)}} \times \frac{1}{t_2 - t_1} \times 100 \quad \text{… (3.9)}$$

The comprehensive land use dynamic degree:

$$S = \frac{\sum_{i=1}^{n} \{LA_{(i,t1)} - ULA_{(i)}\}}{\sum_{i=1}^{n} LA_{(i,t1)}} \times \frac{1}{t_2 - t_1} \times 100 \quad \text{… .(3.10)}$$

The spatial-based land use dynamic degree (the rate of change):

$$CCL_i = TRL_i - IRL_i \quad \text{… (3.11)}$$

$$TRL_i = \frac{LA_{(i,t1)} - ULA_i}{LA_{(i,t1)}} \times \frac{1}{t_2 - t_1} \times 100 \quad \text{… (3.12)}$$

$$IRL_i = \frac{LA_{(i,t2)} - ULA_i}{LA_{(i,t1)}} \times \frac{1}{t_2 - t_1} \times 100 \quad \text{… (3.13)}$$

S_i represents the dynamic degree of a specific land use type, while S represents the comprehensive land use dynamic degree. The area of a particular land use type at an earlier date is denoted as $LA_{(i,t1)}$, and the area of the same land use type at a later date is denoted as $LA_{(i,t2)}$. The unchanged portion is represented by ULA_i. The variables t_1

andt_2 indicate the year before and after the change, respectively. The transfer-out rate is denoted as TRL_i, the transfer-in rate as IRL_i, and the sum of TRL_i and IRL_i as CCL_i

3.6.2 Transition probabilities

The Markov model enabled the prediction of the spatial distribution of individual LULC classes, relying on the transition probability (pij) between each pair of LULC classes (i and j). The calculation of pij for a specific time period, starting at time t and concluding at time tp1, was determined using Equation 3.14.

$$pij = \frac{nij}{nj} \quad \dots (3.14)$$

$$\sum_{j=1}^{k} pij = 1 \quad \dots (3.15)$$

In Equation 3.14, the calculation of the transition probability (pij) involves the variables ni, nij, and k. Here, ni represents the total number of pixels that have undergone changes within class i during the transition period, while nij corresponds to the number of pixels that have transitioned from class i to class j. The value of k represents the total number of LULC classes, and these calculations were performed to derive the transition probabilities

$$\mathrm{p} \times \mathrm{M}_{\mathrm{t}} = \mathrm{M}_{\mathrm{t+1}} \quad \dots (3.16)$$

The initial LULC distribution at time t (Mt) and the matrix of transition probabilities (p) were used in order to project the future dispersal of each LULC class at time t+1 (Mt+1). Calculating the transition matrices between the time periods 2003 and 2013, and 2013 and 2023, using a first-order Markov model, required the use of the LULC maps that were produced as a result of the classification technique for the years 2003, 2013, and 2023. These maps were used in the calculation. These transition matrices were an extremely important component of the many different processes that went into the prediction of LULC shifts.

3.6.3 Model validation

To assess the accuracy of the employed models and facilitate comparisons between them, a crucial step is the calibration and validation process. This step aims to identify changes and determine the model that exhibits the highest level of reliability in predicting future land use changes. As part of the validation stage, the kappa coefficient was computed, which was a commonly used measure to evaluate the predictive capability of a model.

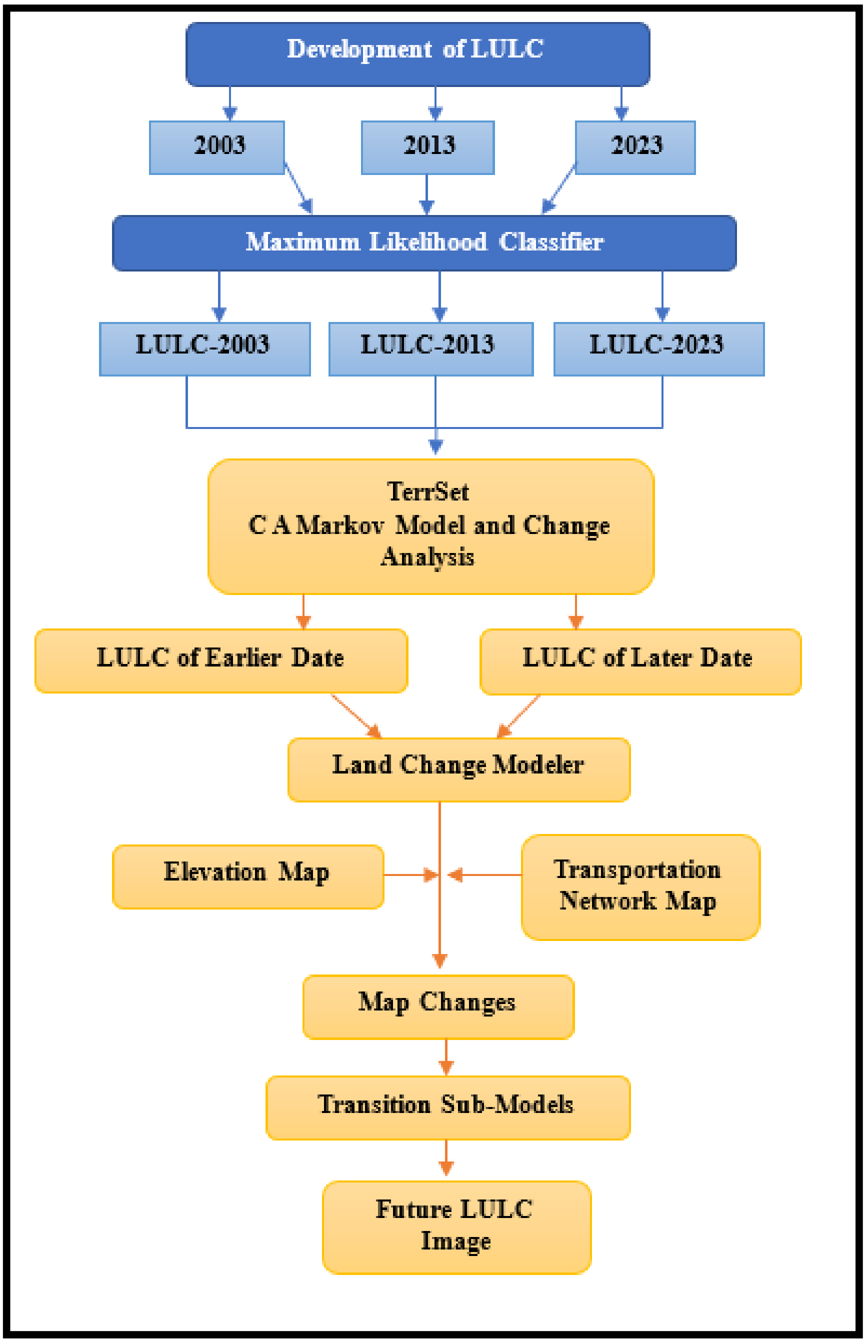

Fig. 3.2 Methodological scheme for LULC classification and future LULC

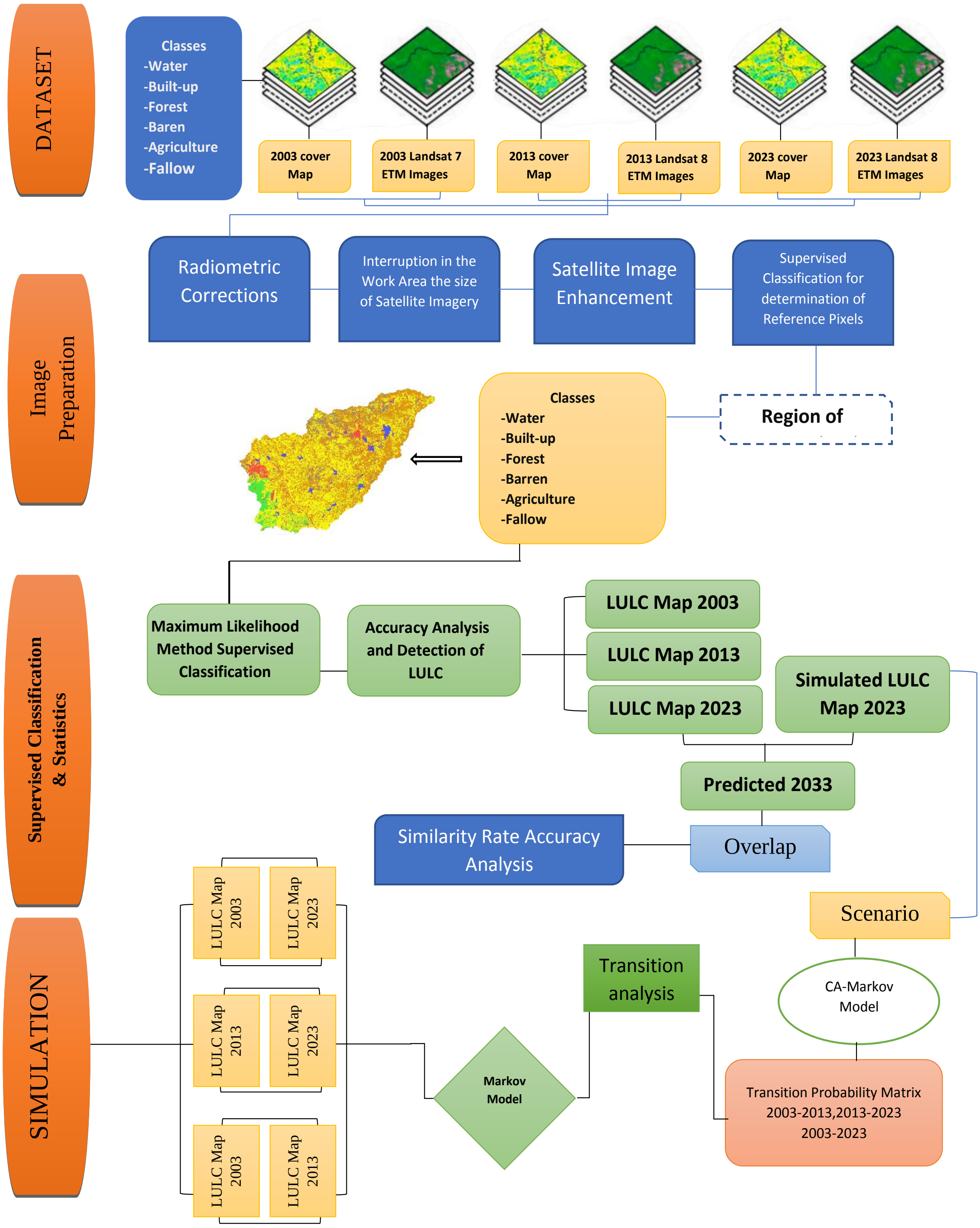

Fig 3.3 Flow Chart of the Modelling Process

3.7 Indices for LULC Change Assessment

3.7.1 Normalized difference vegetation index (NDVI)

The Normalised Difference Vegetation Index (NDVI), which measures the health of the vegetation, is used extensively around the world. The Enhanced Vegetation Index (EVI), Perpendicular Vegetation Index (PVI), and Ratio Vegetation Index (RVI) are few more popular vegetation indices. Vegetation that is healthy and robust typically absorbs visible light across the electromagnetic range. In particular, chlorophyll, which is found in green plants, absorbs blue (0.4–0.5 m) and red (0.6–0.7 m) wavelengths, reflecting the green spectrum (0.5–0.6 m). Because of this, healthy foliage appears green to human eyes. Healthy plants have a high level of reflectivity in the near-infrared (NIR) band, which is between 0.7 and 1.3 m. The interior structure of plant leaves is the main factor affecting this reflectance. These two bands were used in the NDVI calculation by taking into account the high NIR reflectance and the considerable red absorption. Consequently, the normalised difference vegetation index (NDVI) was calculated using the formula below.

$$\mathrm{NDVI} = \frac{(\mathrm{NIR} - \mathrm{Red})}{(\mathrm{NIR} + \mathrm{Red})} \qquad \ldots (3.17)$$

- For Landsat 7 data, NDVI = (Band 4 – Band 3) / (Band 4 + Band 3)
- For Landsat 8 data, NDVI = (Band 5 – Band 4) / (Band 5 + Band 4)

The NDVI value varies from -1 to 1. Higher the value of NDVI is an indicator of high Near Infrared (NIR)reflectivity, means dense greenery.

- NDVI = -1 to 0 represent Water bodies
- NDVI = -0.1 to 0.1 represent Barren rocks, sand, or snow
- NDVI = 0.2 to 0.5 represent Shrubs and grasslands or senescing crops
- NDVI = 0.6 to 1.0 represent Dense vegetation or tropical rainforest

The NDVI rate can be calculated using raster calculator in ArcGIS.

Table.3.5. shows the characteristics for multiple characteristics as well as the wavelength range. In other words, divides by their sum pixel-by-pixel after subtracting the value of the red band from the value of the NIR band. Rock, sand, or snow-covered deserts correspond to very low NDVI values (0.1 and lower). High numbers denote temperate and tropical rainforests (0.6 to 0.8), whereas moderate values imply shrub and grassland (0.2 to 0.3). Water bodies are represented with negative NDVI values, while bare land is represented by NDVI values that are closest to 0.

Table 3.5 Thematic Bands of LANDSAT Satellite

Band	Name of the Band	Wavelength(μm)	Characteristics and Usage
1	Visible Blue	0.45-0.52	Maximum Water Penetration
2	Visible Green	0.52-0.60	Good for Measuring Plant Vigor
3	Visible Red	0.63-0.69	Vegetation Discrimination
4	Near Infrared	0.76-0.90	Biomass and shoreline mapping
5	Middle Infrared	1.55-1.756	Moisture content of soil
6	Thermal Infrared	10.4-12.5	Soil moisture and thermal mapping
7	Middle Infrared	2.08-2.35	Mineral mapping

3.7.2 Normalized difference built-up index (NDBI):

$$BU = NDBI - NDVI \quad \text{… (3.18)}$$

Normalized Difference Vegetation Index (NDVI) and the Normalized Difference Built-up Index (NDBI). These indexes are commonly used in the analysis of urban areas. The indices of interest in this study were the Normalized Difference Built-up Index (NDBI), Built-up Index (BU), and Urban Index (UI). The implementation of index-based image classification techniques, such as supervised and unsupervised classification, can present a challenging and time-intensive undertaking. The process entails the amalgamation of various bands and the execution of multiple operations to derive the ultimate outcome. The efficacy of the image classification methodology is contingent upon the proficiency of the image analyst and the approach utilized. In contrast to other methods, the calculation of Normalized Difference Built-up Index

(NDBI) is considered to be a relatively uncomplicated and direct process. The NDBI calculation formula can be expressed as follows (Equation 3.19).

$$NDBI = \frac{(SWIR - NIR)}{(SWIR + NIR)} \quad \dots (3.19)$$

For Landsat 7 data, NDBI = (Band 5 – Band 4) / (Band5 + Band 4)

For Landsat 8 data, NDBI = (Band 6 – Band 5) / (Band6 + Band 5)

The normalization of the difference is a technique used in data analysis to standardize the difference between two values. The Build-up Index (BUI) is a metric that ranges from -1 to +1. The NDBI metric exhibited a negative correlation with water bodies, while a positive correlation was observed with built-up areas. The Normalized Difference Built-up Index (NDBI) value pertaining to vegetation exhibits a low value.

3.7.3 Normalized difference water index (NDWI)

The utilization of the Normalized Difference Water Index (NDWI) is common in the analysis of water bodies. The utilization of the Green and Near Infrared (NIR) spectral bands extracted from remote sensing imagery was employed in the computation of this index. The Normalized Difference Water Index (NDWI) was been found to be a reliable method for improving the detection and characterization of water bodies. The study suggested that built-up land may cause sensitivity in the estimation of water bodies, which could result in their potential overestimation. The utilization of NDWI products in combination with NDVI change products could be employed to evaluate the context of observable change regions. The visible portion of the electromagnetic spectrum is characterized by low reflectance in water bodies. It was observed that liquid water exhibits greater reflectance in the Blue spectra (0.4 - 0.5 µm) in comparison to the Green (0.5 - 0.6 µm) and Red (0.6 - 0.7 µm) spectra. The reason behind the blue color of water was the subject of investigation. It was observed that water with high turbidity levels exhibited increased reflectance within the visible spectrum. Water exhibited minimal reflection in the Near Infrared (NIR) and longer wavelengths. The Normalized Difference Water Index (NDWI) can be computed by applying the subsequent mathematical expression.

$$NDWI = \frac{(NIR - SWIR)}{(NIR + SWIR)} \quad \ldots (3.20)$$

- For Landsat 7 data, NDWI = (Band 4 – Band 5) / (Band 4 + Band 5)
- For Landsat 8 data, NDWI = (Band 5 – Band 6) / (Band 5 + Band 6)

But result appear form above formula is poor in quality. The pure water neither reflects NIR nor SWIR. The formula of NDWI then modified by Xu (2005). It uses Green and SWIR band.

$$NDWI = \frac{(Green - SWIR)}{(Green + SWIR)} \quad \ldots (3.21)$$

- For Landsat 7 data, NDWI = (Band 2 – Band 5) / (Band 2 + Band 5)
- For Landsat 8 data, NDWI = (Band 3 – Band 6) / (Band 3 + Band 6)

Similar to this, the value of the Normalize Difference Water Index (NDWI) ranges from -1 to 1. NDWI values for water bodies are often higher than 0.5. Vegetation has substantially lower values, making it simple to identify it from bodies of water. Positive build-up characteristics range from 0 to 0.2.

Results and Discussion

4.1 Generation of Land use and Land cover (LULC) Map

Individual land use and land cover (LULC) categories in this research area were identified and mapped using a combination of remote sensing and field observations. The identification process was based on False Colour Composite (FCC) images extracted from Landsat-7 and 8 (ETM+/OLI) satellite data and created LULC using Arc GIS (10.4.1). Distinct colors were used by the FCC to represent different land covers. For instance, bright red was used to display dense forest cover, black was used for water bodies and so on (Table 4.1).

Table 4.1: Characteristics of land cover classes

Land use classes	Description	Characteristics on Landsat False Color Composite (FCC)
Built up	Settlements including Roads and concrete structures	Different shades of Cyan
Water body	Ponds, lakes, canals, dams etc.	Dark bluish to black
Forest	Tree cover	Red
Barren land	Open fields, exposed lands and sand fill areas	White
Agricultural land	Crop fields	Yellow
Fallow	Agricultural field without crops	Orange

Remote sensing and GIS techniques were used to produce LULC maps. The visual representation of the land use categories on the maps was facilitated by assigning each category a specific color. Forest cover was denoted by green colour, agricultural land was represented by yellow, water bodies were indicated by blue, fallow land was denoted by tangerine, built-up areas were signified by red and barren land was depicted by dove colour. Doddahalla watershed was opted as Region of Interest (ROI), selected for conducting supervised classification on Landsat 7 ETM and landsat 8 OLI LISS III satellite data. Land use and land cover features like forest, agricultural land, built-up areas, water bodies and barren land were trained using ArcGIS (version 10.4.1). The entire image was divided into separate classes during the maximum likelihood classification process. The training sites were selected from areas that were relatively homogeneous to ensure that they accurately represented each land cover class. The classification algorithm underwent training using signatures extracted from the image. The image processing software accurately assigned selected pixels to their respective classes based on distinct characteristics possessed by the training data in supervised classification **(Nair *et al.*, 1993)**. The production of classified maps resulted from this approach gave valuable insights into the geographic distribution and extent of the various land use and land cover classifications within the Doddahalla study area.

4.2 Temporal Changes in Land Use and Land Cover Class Map

The dynamics of land use were examined through the utilisation of visual interpretation and digital satellite data analysis obtained from the USGS Earth Explorer website. The study was concentrated on the temporal range spanning from 2003 to 2023. The study analysed land use changes in order to evaluate the differences in land use classifications over various time periods. Fig. 4.2 presents the percentage change in land area for each land use category, as obtained from the results.

Following the implementation of supervised classification, statistical analyses were conducted to determine the distribution of land cover classes. Subsequently, the extent of land use categories was estimated for the years 2003, 2013 and 2023 (Fig. 4.1). The geographical area under study was analysed to determine the variations in forest, builtup, fallow, water, agricultural and barren land areas for selected years. The forest area changed from 269.13 km^2 to 489.82 km^2, the builtup area varied from 16.14 km^2 to 72.95 km^2, the fallow land area changed from 360.32 km^2 to 380.73 km^2, the water area varied from 5.85 km^2 to 19.10 km^2, the agricultural land area changed from 269.13 km^2 to 489.82 km^2, Lastly, the barren land area varied from 319.76 km^2 to 70.19 km^2 from year 2003 to 2023 respectively.

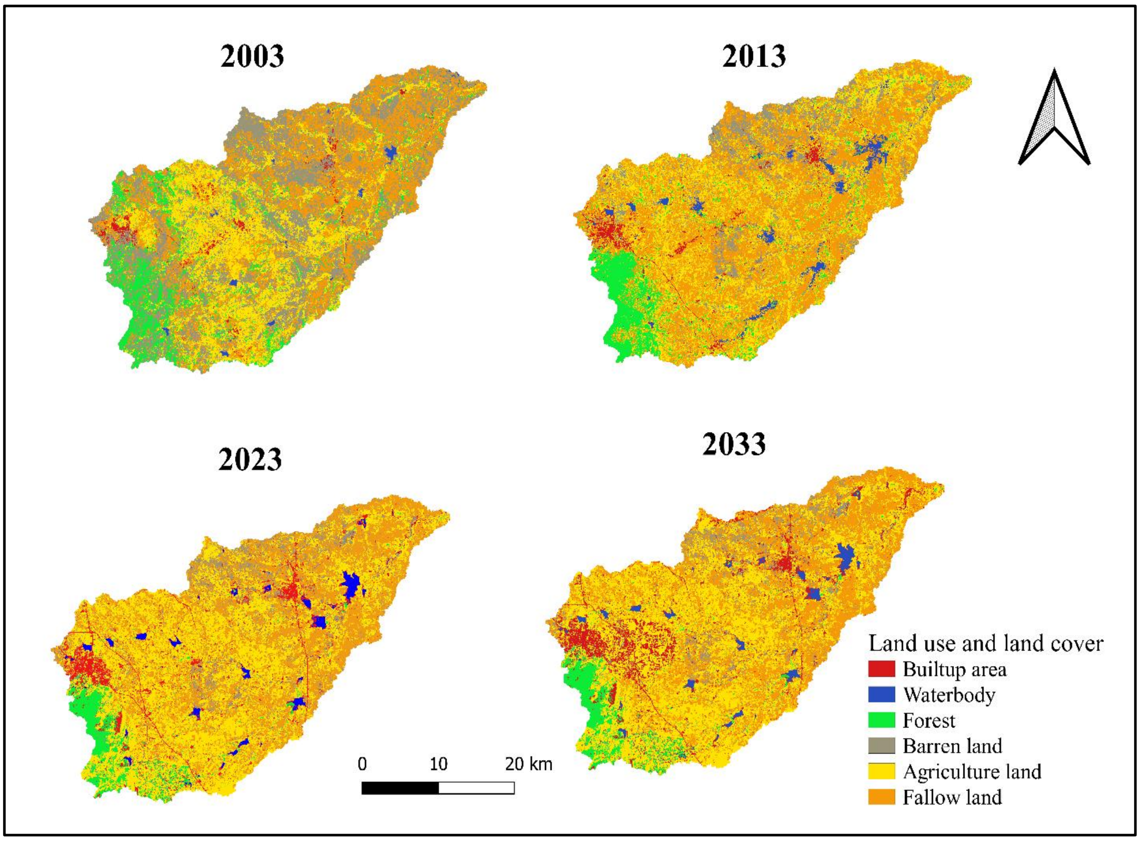

Fig. 4.1 Temporal Analysis of Land Use and Land Cover from 2003-2033

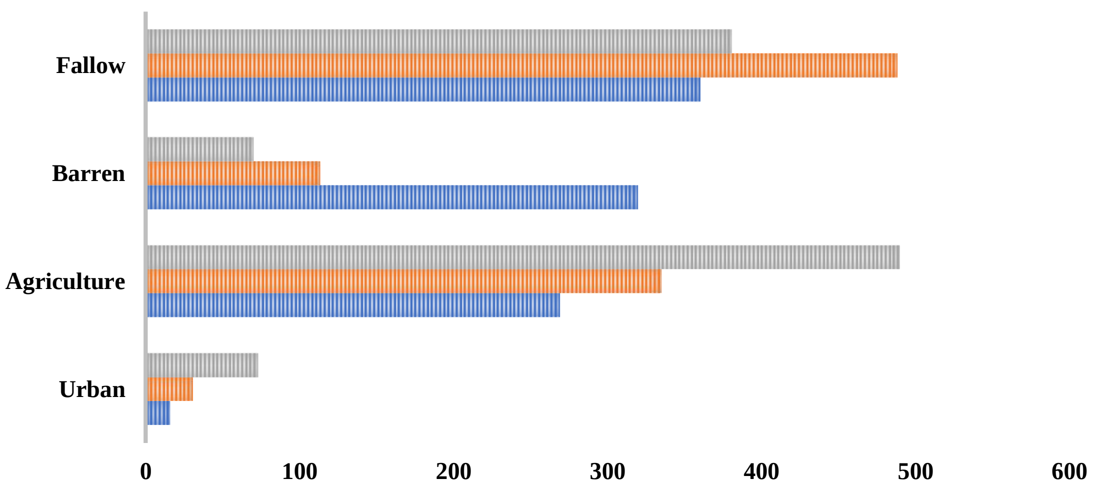

	Urban	Agriculture	Barren	Fallow
2023	72.95	489.82	70.19	380.73
2013	30.58	335.1	113.42	488.41
2003	16.14	269.13	319.76	360.32

Fig. 4.2 Decadal variation in Land Use of the Doddahalla Watershed

4.2.1 Forest Area

The Doddahalla watershed is a region of ecological significance, recognised for its diverse flora and fauna. It is situated in an area of notable environmental importance. The forest cover in the watershed has been observed to undergo a concerning reduction over time. The purpose was to conduct an examination of the forest's region located in the Doddahalla watershed. The analysis focused on the observed pattern over the last 20 years, utilising data collected from 2003, 2013 and 2023.

The data collected for the years 2003, 2013 and 2023 revealed a consistent and concerning trend of decreasing forest area within the Doddahalla watershed. In 2003, the total forest area was measured as 116.79 km^2, decreased to 95.99 km^2 in 2013. The most recent data from 2023 indicates a further decline, with the forest area shrinking to 55.26 km^2 as represented in Fig. 4.3

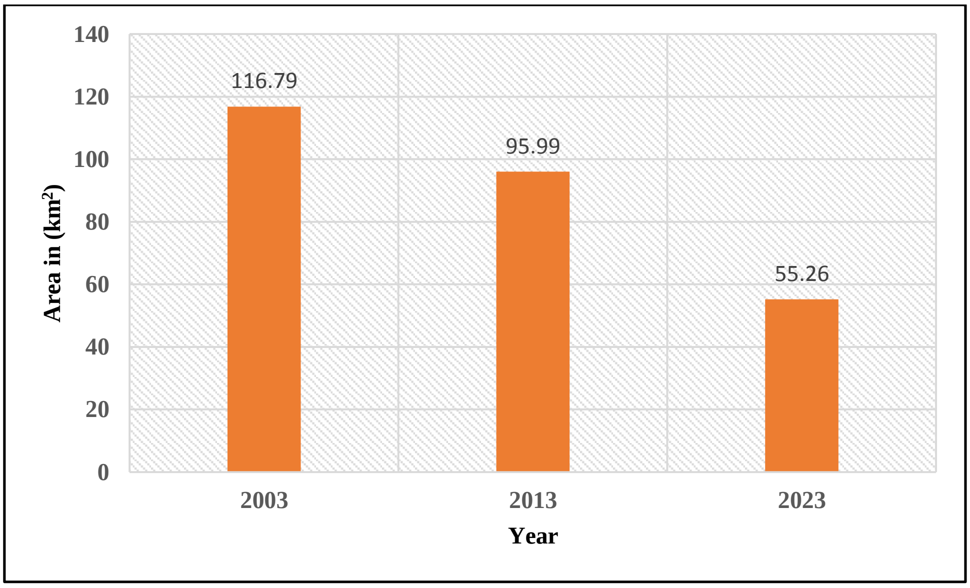

Fig. 4.3 Variation in area of forest during the period from 2003-2023

4.2.2 Agricultural land

The Doddahalla watershed is a noticeable agricultural area known for its rich soil and advantageous climate The present study provide an examination of the agricultural region situated in the Doddahalla watershed. The report focused on the observed pattern over the last twenty years, utilising data from the years 2003, 2013 and 2023.

The analysis of the data gathered from the Doddahalla watershed for the years 2003, 2013 and 2023 indicated a persistent and significant pattern of growth in the agricultural area. The agricultural land area was quantified at 269.12 km^2 in 2003 and increased to 335.10 km^2 by 2013. According to the latest data obtained in 2023, there has been a notable expansion in the agriculture area, which now covered about 487.82 km^2 (Fig. 4.4). The increasing trend in agricultural land use observed within the Doddahalla watershed indicates the region's growing agricultural activities and their significant contribution to the local economy.

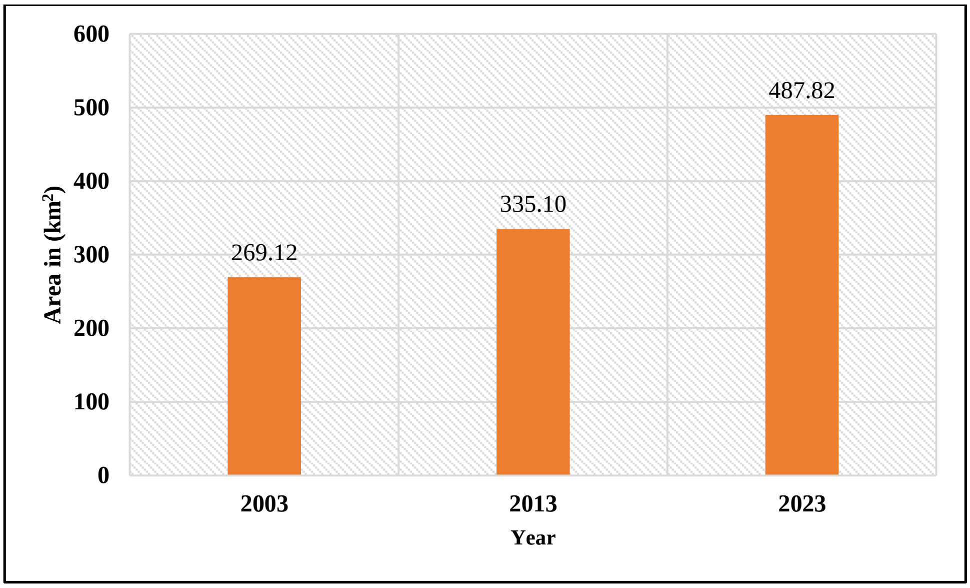

Fig. 4.4 Variation in area of Agriculture land during the period from 2003-2023

4.2.3 Fallow Land

A curious trend was observed in the fallow land use classification within the Doddahalla watershed, based on the findings of this study. It indicated that there was a significant increase in the area designated as fallow land from 360.33 km^2 in 2003 to 488.19 km^2 in 2013. It is worth noting that a decrease in the area of fallow land was observed in the year 2023, with an extent of 380.73 km^2 (Fig. 4.5). The observed notable rise between 2003 and 2013 indicates a possible alteration in land management techniques and agricultural approaches during the aforementioned timeframe **(Gulati and Rai, 2015).**

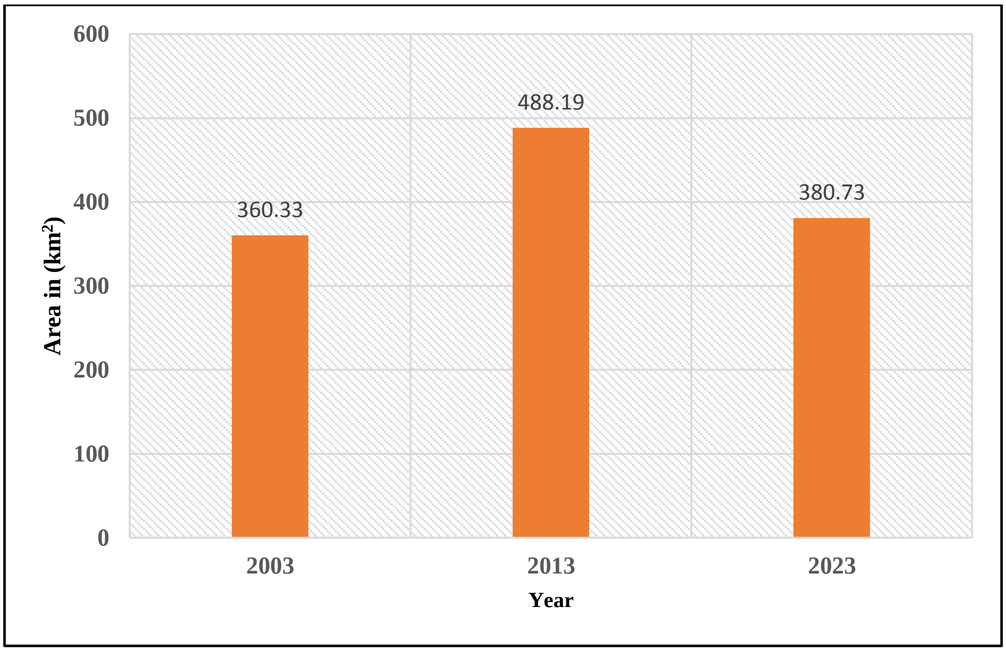

Fig. 4.5 Variation in area of fallow land during the period from 2003-2023

4.2.4 Built up area

The findings also revealed major changes in the built-up and forest regions within the study area, with the rapid rise of human settlement being the primary driver of these changes. fluctuations in the built-up area were noticed during the course of the twenty-year period beginning in 2003 and ending in 2023. These fluctuations were a direct result of the development of new buildings, roads and other types of infrastructure **(Adepoju and Salami, 2017)**. Built-up area covered 16.14 km^2 in 2003, 30.58 km^2 in 2013 and 72.95 km^2 in 2023 (Fig. 4.6). The ever-increasing requirements of a growing human population could be credited with driving the unabated expansion of the built-up area during the entirety of the research period. The increased value of the built-up land area in 2023 in comparison to preceding years was indicative of the increased level of construction activity that took place in the interim years. This meant that more buildings and roads were created in order to accommodate the population growth and meet the increasing demands that urbanisation had brought forth.

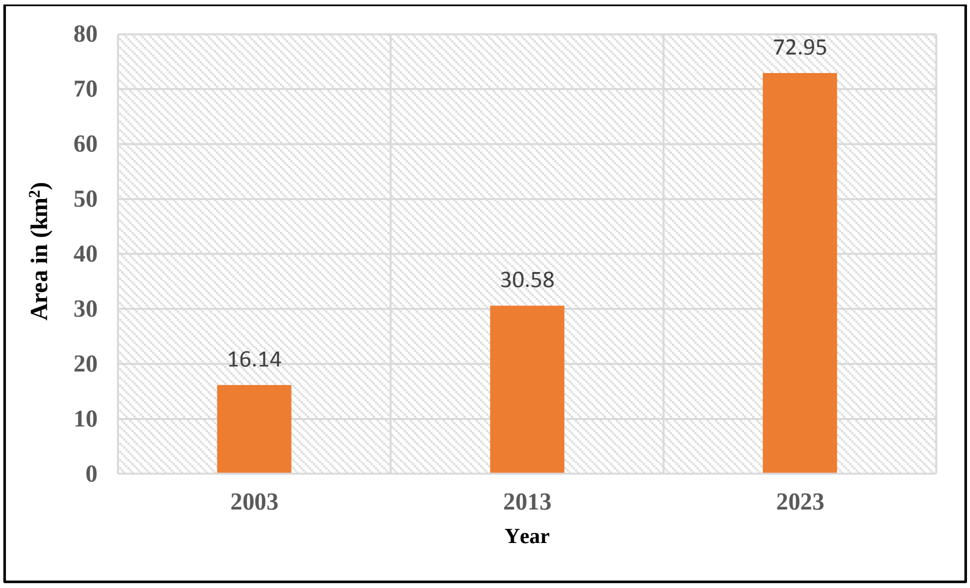

Fig. 4.6 Variation in area of builtup land during the period from 2003-2023

4.2.5 Water

The present study employed a Land Use and Land Cover (LULC) analysis to examine alterations in the water area of the Doddahalla watershed in Chitradurga district over the course of 20 years, from 2003 to 2023. The results of the study offered significant contributions to the understanding of water availability patterns in the area, specifically during a prolonged drought episode spanning from 2002 to 2006.

The findings indicate that in the year 2003, the water area within the watershed exhibited a statistically significant decrease, measuring 5.84 km$^{2.}$ The observed reduction in the measured variable could be assigned to the persisting effects of the intense drought event, which exerted a discernible impact on the hydrological parameters throughout the corresponding period.

By contrast, the year 2013 exhibited a significant rebound, as the water area increased to 24.46 km^2. The observed positive shift indicated the resilience of the region and its potential for rehabilitation of water resources subsequent to the prolonged drought. The recovery observed in this study could potentially be attributed to a range of factors, such as enhanced precipitation trends etc. But in 2023, decrease in the water area was observed, with measurements indicating a value of 19.10 km$^{2.}$ The observed reduction, might suggest alterations in the ecological circumstances or human-induced impacts in the catchment area. **Fig. 4.7** represents the area of water present in watershed in km^2.

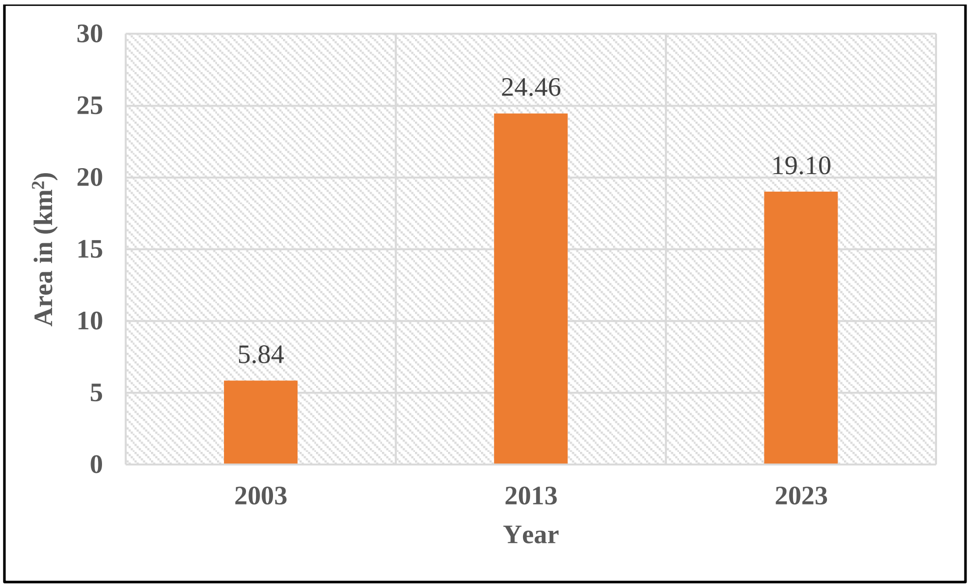

Fig. 4.7 Variation in area of water during the period from 2003-2023

4.2.6 Barren Land

The alterations in the extent of barren land in the Doddahalla watershed of Chitradurga district, spanning a duration of two decades, namely 2003 to 2013 and 2023 were examined. The delineation of the areas was carried out via a rigorous Land Use and Land Cover (LULC) analysis. The findings offered significant contributions to the understanding of land use change patterns, specifically the transformation of unproductive land into developed zones adjacent to roads.

According to the results, the extent of unproductive land within the watershed was recorded as 319.75 km^2 during the year 2003. The potential causes of this vast area of unproductive land might be impacted by a range of factors, including natural phenomena, land degradation, or land management techniques that were in use during the period in question.

In 2013, a notable decrease in the extent of barren land was observed, with a recorded reduction to 113.42 km$^{2.}$ The observed reduction indicated a transformation of unproductive land into alternative land use categories, predominantly agricultural and builtup land uses. In 2023, a comprehensive analysis indicated a persistent decline in the extent of barren land. The current measurement of the barren land area was 70.19 km^2 (Fig. 4.8). The observed trend indicated a continuous alteration in land use, characterised by further transformation of unproductive land into alternative categories.

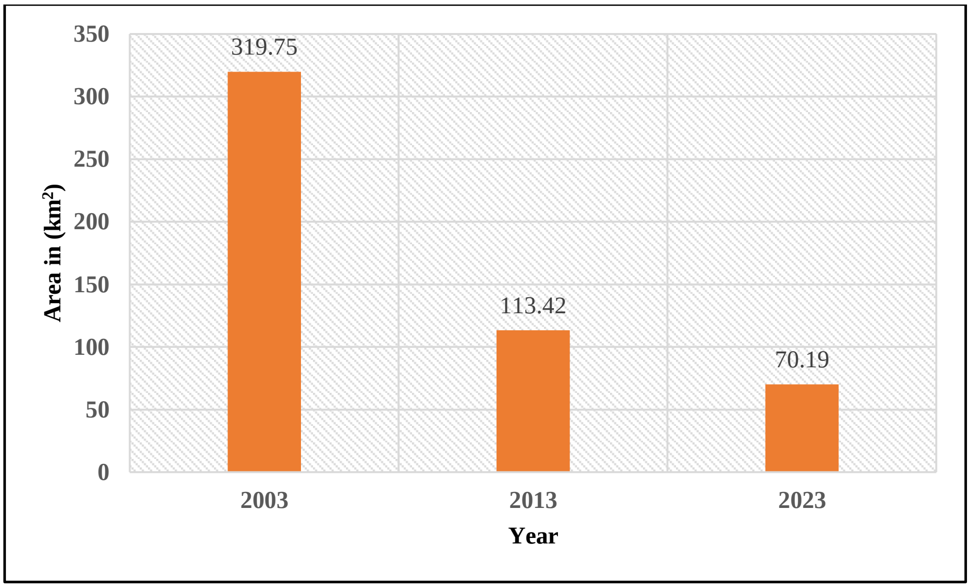

Fig. 4.8 Variation in area of Barren land during the period from 2003-2023

4.3 Key Drivers used for prediction of LULC for the year 2033

The Land Use and Land Cover (LULC) map for the year 2033 was predicted by utilizing four significant drivers, namely slope, elevation map, Euclidean distance map (builtup) and road maps. Drivers such as these are utilized in LULC modeling to gain insight into and forecast alterations in land cover configurations **(Schulz *et al.*, 2011)**. The process that was followed using the TerrSet software involved integrating the drivers and applying appropriate analysis techniques.

The steepness of the terrain, a slope, had the potential to affect the types of land cover present. The slope values were provided ranged from 0 to 49.22. Limited vegetation or less favorable land uses were found on steeper slopes, while flatter slopes might be more appropriate for agriculture, settlements, or other land cover classes.

The elevation map, measured in meters, was used as another important driver in the analysis. The impact of elevation on land cover patterns was a result of its influence on climate, vegetation types and human settlement. The range of elevation values obtained were from 516.24 to 1131.75 meters. The distribution of land cover classes may vary with elevation, where forests or other natural land cover classes tend to occur at higher elevations, while agricultural or builtup areas were more commonly found at lower elevations.

The proximity of builtup areas to each location was represented using the Euclidean distance map. It was found that Euclidean distance could be used as a measure of straight-line distance to quantify the distance to builtup areas. The addition of this driver in the analysis allows for the influence of development on land cover change to be accounted for. The data provided ranged from 0 to 2120.86 meters, indicating the proximity of the locations to builtup areas, with shorter distances indicating closer proximity.

Finally, the road map was employed for predicting land cover. The role of road networks in land use patterns was significant as they determined accessibility and human activities. The impact of road information on land cover change was considered in the study. The range of Euclidean distance values provided by the study was from 0 to 3973.16 meters. Shorter distances were indicative of closer proximity to road infrastructure.

Spatial analysis techniques such as regression or machine learning algorithms were most likely employed using the TerrSet software (19.0.5) to model the relationship between the drivers and the observed historical land cover data. A prediction map for the year 2033 was generated by analyzing the relationships using software. The map take into account the potential impact of these drivers on the distribution of land cover classes in the future.

The variability of the modeling process and techniques employed in TerrSet might depend on the particular methodology implemented. The overall methodology entails the incorporation of drivers, examination of their associations with past land cover information and production of a projected LULC map for the future using these associations. Map of key drivers used for prediction are displayed in Fig. 4.9.

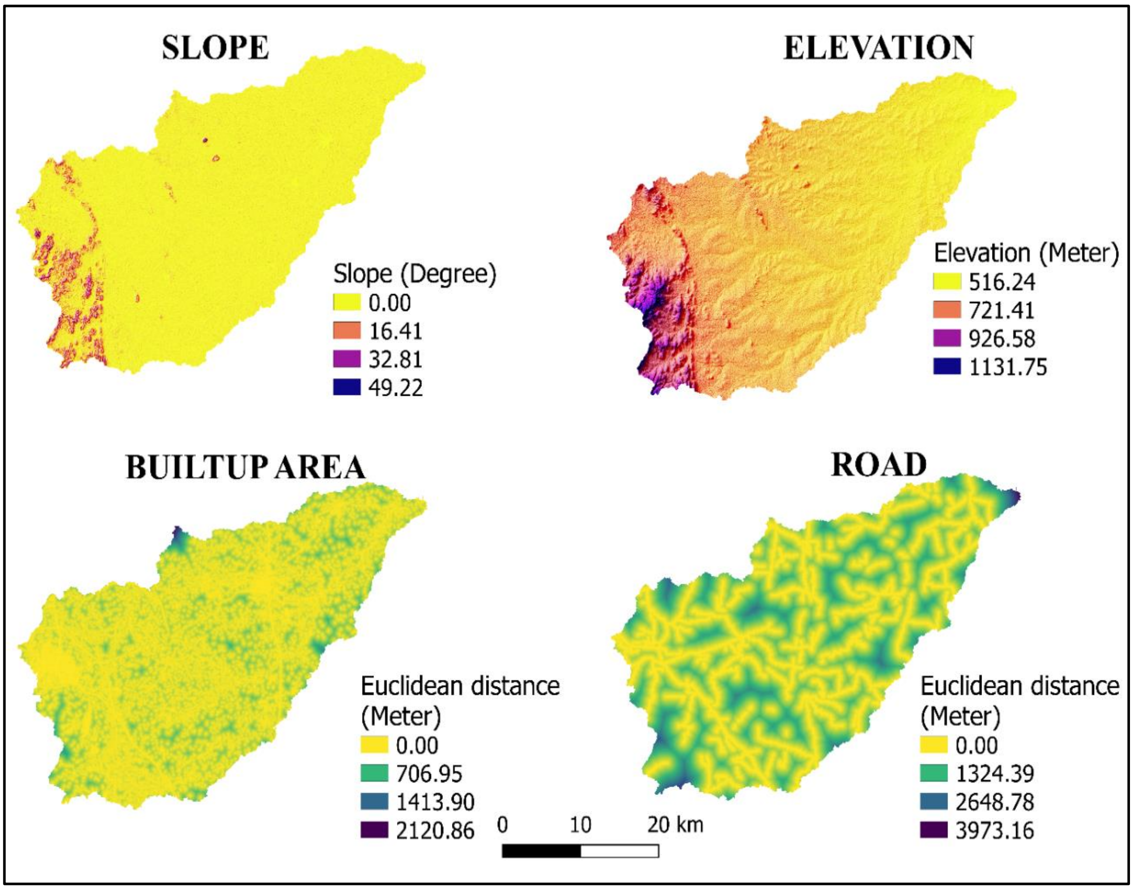

Fig. 4.9 Map of drivers used prediction of future LULC

4.4 Simulation of LULC Change Using Markov Chain Analysis (CA-Markov) Model

Land use and land cover (LULC) for the year 2033 were projected using the CA-Markov model, based on the available data on LULC from 2013 and 2023. The simulated land use fields were compared with the actual current land use within the watershed to validate the forecasted LULC. The model's performance was evaluated using the Kappa index through a comparison, allowing for an assessment of its effectiveness. The accuracy and reliability of the CA-Markov model in predicting LULC changes were evaluated by comparing the observed and simulated LULC for 2023 (Fig. 4.10) **(Jokar *et al.*, 2013).**

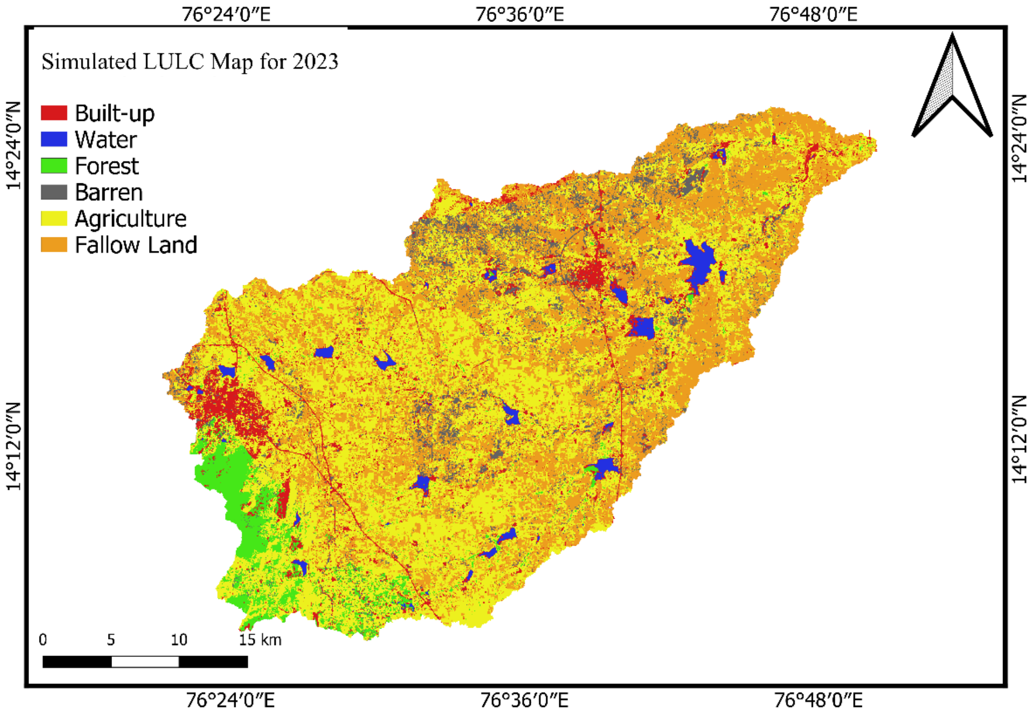

Fig. 4.10 Simulated LULC map for the year 2023

Table 4.2 Transition matrix of future LULC prediction for year 2033

	Built up	**Water**	**Forest**	**Barren**	**Agriculture**	**Fallow**
Built up	0.4296	0.0148	0.0265	0.0100	0.3224	0.0000
Water	0.0000	0.2374	0.0615	0.0232	0.3929	0.0200
Forest	0.0000	0.0064	0.1327	0.0309	0.5494	0.0200
Barren	0.5000	0.0112	0.0232	0.1013	0.4012	0.0200
Agriculture	0.0000	0.0096	0.0338	0.0478	0.5057	0.0200
Fallow	0.0500	0.0105	0.0298	0.0560	0.4654	0.0000

4.5 Land Use and Land Cover Prediction

The predicted scenarios for the year 2033 (Fig. 4.11) was analysed based on a research study that used a Markov-CA prediction model. The MLP method reported an accuracy of 64% for the model **(Sundara *et al.*, 2015)**. A single transition scenario was generated by focusing the predictions on changes within the Built up and occupied classes. The expected changes in the map would only be seen in the built-up category. There had been an increase in urbanisation along newly constructed roads developed since 2013. The spatial distribution of builtup areas in the predicted map seemed to have been significantly influenced by these roads. Different changes in the landscape were observed during the period spanning from 2023 to 2033. The transition trend shown in the Markov Chain transition matrix could be utilised to observe the above alterations. The matrix displays the probabilities linked with the shifts from one land cover category to another (Table 4.2). Through the examination of the transition matrix values, insights regarding the probability of a particular land cover category transitioning to another category could be obtained. The probabilities presented in the analysis offered significant insights into the land cover change dynamics of the investigated region **(Kamaraj *et al.*, 2017)**

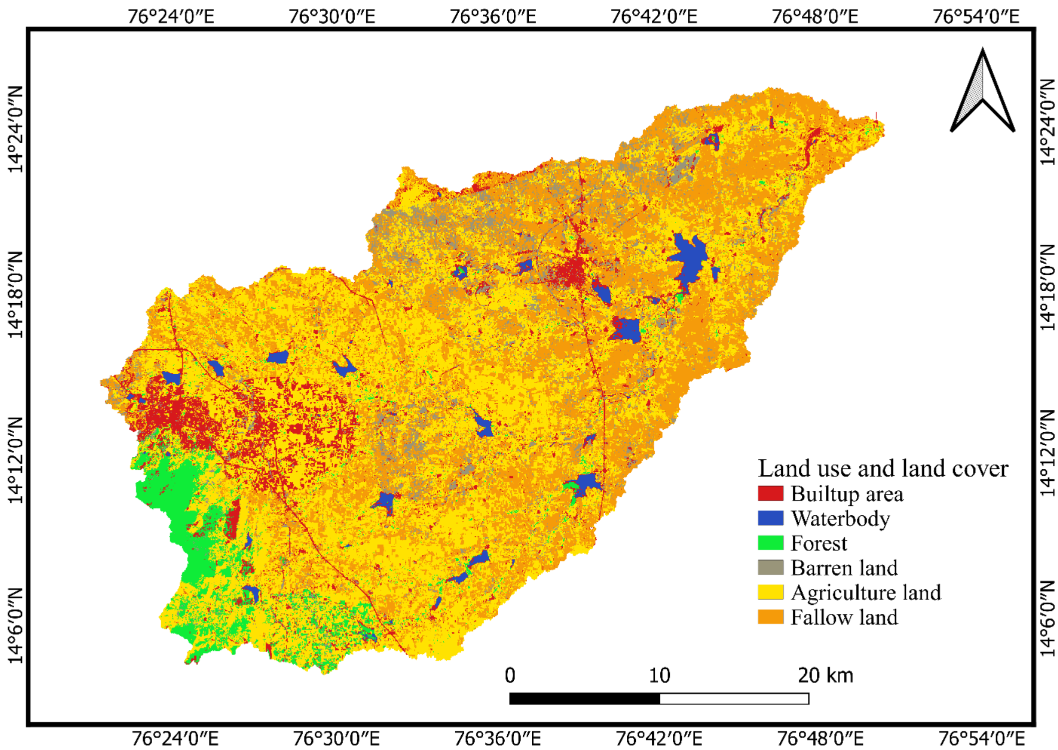

Fig. 4.11 Predicted LULC map for year 2033

The identification of suitable drivers for predictive modelling was a critical component in projecting potential results. It was important to identify the key drivers that had a substantial impact on the patterns and trends of land use and land cover change

(LULC) in the designated study region. Three variables were selected based on their significance. The driver variables considered in this study comprised of slope, elevation, built-up Euclidean distance, road Euclidean distance and the probability of transformation from barren land to built-up areas, as well as from fallow land to built-up areas. The driver variables were subjected to careful consideration and subsequently integrated into the predictive model.

4.5.1 Gains and losses occurred in LULC

The built-up area within the area under study found significant increase over time. This observation was consistent with the transition matrix, which showed that a sizeable part of fallow and barren land from the various land cover classes had undergone transformation into the built-up class. A new area has also been transformed into a built-up area. These results demonstrate the ongoing urbanisation and growth of populated places in the research area.

According to the results, it was projected that urban areas would cover approximately 95.49 km^2. This indicated a significant increase in built-up areas compared to the current scenario. In 2033, water bodies were estimated to cover approximately 19.1 km^2, suggesting that water resources remain relatively stable. Monitoring and conserving water bodies was essential for sustainable water management and to address potential water scarcity issues. The forested areas were projected to cover around 55.26 km^2, indicating a slight decline from the present condition. The reduction in forest cover was primarily caused by deforestation, land conversion for agriculture or urban expansion and natural disturbances. The projected area of barren lands, which were characterised by limited vegetation cover, is approximately 66.68 km^2. The estimated extent of agricultural land in the region was approximately 489.82 km^2, highlighting the ongoing significance of agriculture. Ensuring sustainable agricultural practices, such as soil conservation, water management and the adoption of climate-smart agriculture techniques, was found crucial for mitigating potential environmental impacts and enhancing agricultural productivity. The projected coverage of fallow lands was approximately 361.69 km^2, representing areas that were temporarily or partially left uncultivated.

The predicted land use and land cover changes for 2033 showed a dynamic landscape influenced by urbanisation, agricultural activities, environmental factors and socio-economic dynamics. The findings emphasised the importance of sustainable land management, integrated planning approaches and policy interventions in tackling the challenges related to land-use changes and achieving a harmonious balance between development and conservation.

4.5.2 Parameters and performances of the model

Applying a design of neural networks with 4 input layer neurons, 7 hidden layer neurons and 8 output layer neurons, TerrSet software was used to create the prediction model. A dataset with 5266 desired samples for each class was utilized to train the model. 10,000 rounds of training were performed, with a final learning rate of 0.0001 and a momentum factor of 0.5. Set to 1, the sigmoid constant.

After the model had been trained, its performance was assessed using a number of measures. The model was successful in fitting the training set of data, as seen by the training RMS's value of 0.3281. The testing RMS came up with a somewhat higher result of 0.3285, indicating that the model performed quite well in terms of applicability. The model's accuracy rate, which gauged how well it could predict the LULC classes, was found to be 63.49%. Although this accuracy rate may seem low, it should be emphasized that predicting land cover can be difficult due to a number of reasons, including complicated land dynamics and data input uncertainties.

Furthermore, the model's capacity to anticipate events beyond chance was shown by the skill measure of 0.0968. The CA Markov model has the potential to capture certain underlying patterns and trends in LULC changes, despite the skill measure's modesty.

4.6 Validation of Model

Actual and simulated LULC were built for the year 2023 (Fig. 4.11). As a result, slight modifications had been seen for other LULC classes, while the forest cover was shown to be strikingly similar in both real and simulated maps of the year 2023. All land use and land cover classes had the best range of agreement with a rate of variation under 10% according to the area covered by the two maps. The Kappa Index of Agreement

(KIA) was used to compare the simulated and actual LULC maps for 2023 in order to validate the model.

Two basic models for predicting future scenarios, a hard prediction model and a soft prediction model, were offered by the change allocation panel used in this study. The soft prediction model was preferred in this study because it could create a vulnerability map that would evaluates the probability of change for specific transitions. Specific assumptions were made to model future scenarios for the year 2033 in the watershed. A similar pattern to the observed LULC changes between 2003 and 2013 was assumed to be followed by the nature and developments within the Doddahalla watershed during the modelling process. The transformation weights needed for the Markov Chain probabilities matrix were assessed using Markov Chain analysis. This served as the foundation for creating the potential projection map.

4.7 Indices for LULC Change Assessment

4.7.1 Temporal analysis of builtup development using NDBI

The Normalized Difference Built-up Index (NDBI) was a commonly employed method in remote sensing for evaluating land development and urbanization **(Kshetri 2018).** The present investigation involved the acquisition of NDBI values through Landsat satellite imagery for the years 2003, 2013 and 2023, with a specific emphasis on the Doddahalla watershed situated in the Chitradurga district.

By analysis of Landsat-7 ETM data the Normalized Difference Built-up Index (NDBI) values for the year 2003, was found spanning from -0.31 to 0.55. The observed values indicate an uneven distribution of developed and undeveloped regions throughout the hydrological basin. The presence of non-built-up land cover types, such as vegetation or bare soil, was indicated by negative values, such as -0.13 and -0.03. Conversely, it could be concluded that values that were positive, such as 0.26 and 0.55, were indicative of the presence of developed regions, such as builtup settlements or infrastructure.

In the year 2013, the Normalized Difference Built-up Index (NDBI) exhibited a range of values spanning from -0.33 to 0.25 by computing Landsat 8 OLI data. Upon comparison of the aforementioned values with those obtained in 2003, a marginal rise in the expanse of developed regions within the hydrological basin could be discerned. The study findings indicate that negative values (-0.33 and -0.13) were indicative of the presence of non-built-up land cover types, while positive values (0.06 and 0.25) suggested the expansion of built-up areas and urbanization.

In the year 2023, the Normalized Difference Built-up Index (NDBI) exhibited a range of values between -0.40 and 0.55. The observed values suggested a persistence of the trend noted in 2013, characterized by an increased rate in developed regions. The obtained results indicate that negative values, specifically -0.40 and -0.08, were indicative of the existence of non-built-up land cover in the Doddahalla watershed. Conversely, positive values, such as 0.23 and 0.55, were suggestive of urbanization expansion and intensification within the same area. Temporal Variation of NDBI Values (2003, 2013 and 2023) in the Doddahalla Watershed are shown in Fig. 4.12.

The results of the study indicate a persistent pattern of urbanization and growth of built-up regions in the Doddahalla watershed of Chitradurga district, as evidenced by the analysis of NDBI values spanning two decades. The results of this study emphasize the necessity of implementing efficient land management tactics and sustainable urban planning in order to tackle the environmental and socio-economic difficulties those emerge as a consequence of swift urbanization.

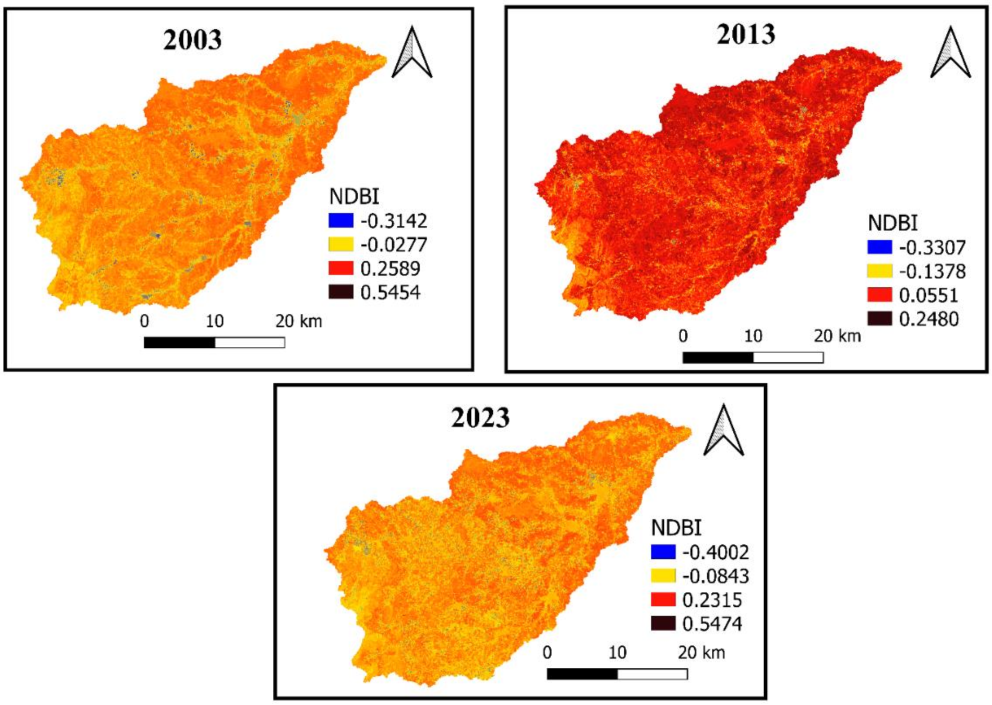

Fig. 4.12 Temporal Variation of NDBI maps of 2003.2013 and 2023

4.7.2 Temporal analysis of vegetation using NDVI

Vegetation health and density could be assessed using the Normalized Difference Vegetation Index (NDVI), which was a commonly used remote sensing index **(Kshetri, 2018).** NDVI values were obtained from Landsat satellite images for the years 2003, 2013 and 2023 in the study.

As in Fig. 4.13, a range of NDVI values from -0.14 to 0.45 were observed during the year 2003. Insights into the vegetation cover within the study area could be obtained from these values. The presence of non-vegetated land cover, such as bare soil or water bodies, could be suggested by negative values, like -0.13. Presence of vegetation was indicated by positive values, including 0.06, 0.25 and 0.45. The vegetation cover can range from sparse or low-density to denser and healthier vegetation cover and these values can be associated with different vegetation types. Areas with higher NDVI **(USGS, 2010)** values indicate the presence of healthier and more abundant vegetation, such as forests, agricultural fields, or well-maintained green cover.

In 2013, the NDVI values ranged from -0.18 to 0.54. Variations in vegetation density and health could be observed when comparing these values with those from 2003. Non-vegetated land cover was still present in the watershed as indicated by the negative values. On the other hand, the positive values (0.06, 0.30 and 0.54) suggest that vegetation cover persisted within the watershed. An improvement in vegetation health and density were indicated by higher NDVI values in 2013 compared to 2003. Various factors, including reforestation efforts, land management practices, or natural regrowth of vegetation, could be attributed to this improvement.

The NDVI values ranged from -0.09 to 0.51 in 2023. The current state of vegetation in the Doddahalla watershed was reflected by these values. Non-vegetated areas were represented by negative values, whereas positive values indicated the presence of vegetation cover. The vegetation status appeared to be relatively stable as the range of NDVI values in 2023 was similar to that of 2013. At a local scale, changes in vegetation density or health can be investigated in specific areas. Vegetation cover within the watershed persisted over the three-year period, as indicated by positive NDVI values. This underscored the significance of preserving and managing these areas to maintain ecosystem services, biodiversity and environmental health.

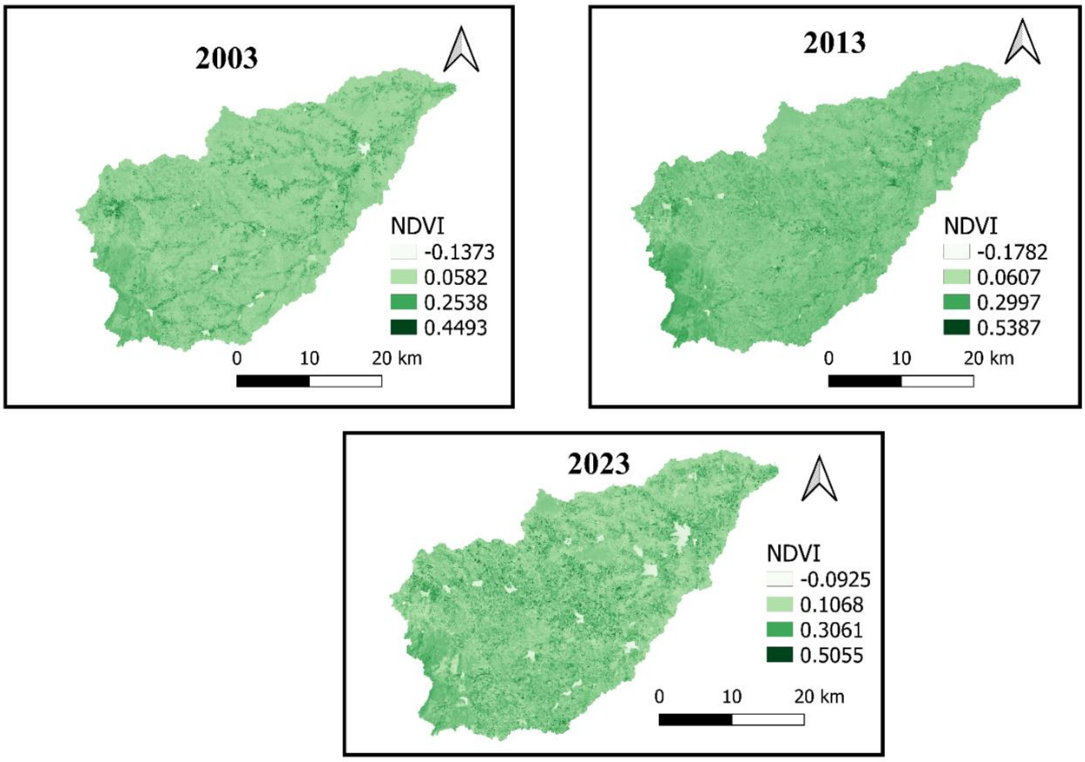

Fig. 4.13 Temporal Variation of NDVI Maps of 2003, 2013 and 2023

4.7.3 NDWI-based temporal analysis of water bodies

The Normalised Difference Water indicator (NDWI), a widely used remote sensing indicator, was used to determine the number and size of water bodies present in a given area **(Kshetri, 2018).** This study focused on the Doddahalla watershed in the Chitradurga district and used NDWI data from Landsat satellite pictures taken in 2003, 2013 and 2023 (Fig. 4.14).

The NDWI values for the year 2003 ranged from -0.44 to 0.11 based on Landsat 7 ETM data analysis. The presence of non-water areas, such as land or vegetation, were suggested by negative values (-0.44 and -0.26). Presence of water bodies, such as rivers, lakes, or reservoirs were indicated by positive values like 0.07 and 0.11. Identification of areas with high water concentration was crucial for comprehending hydrological dynamics and managing water resources in the watershed.

The NDWI values ranged from -0.50 to 0.17in the year 2013. Changes in the extent and distribution of water bodies could be observed by comparing these values with those from 2003. Non-water features were still present in the negative values. The negative values, like -0.50 and -0.28, indicated a change or decrease in water coverage in the watershed. Water bodies might still be present, albeit to a lesser extent than in 2003, even with less negative values like -0.05 and 0.16. The changes observed in the watershed could be due to hydrological variations, land use changes, or climate patterns that impacted the availability and distribution of water resources.

In 2023, the NDWI values ranged from -0.54 to 0.11. The current state of water bodies within the Doddahalla watershed is reflected by these values. Non-water features are present as indicated by negative values (-0.54 and -0.32), while the presence of water bodies is suggested by a positive value of 0.1173. The NDWI values range in 2023 suggested a possible decrease in water coverage when compared to 2003 and 2013.

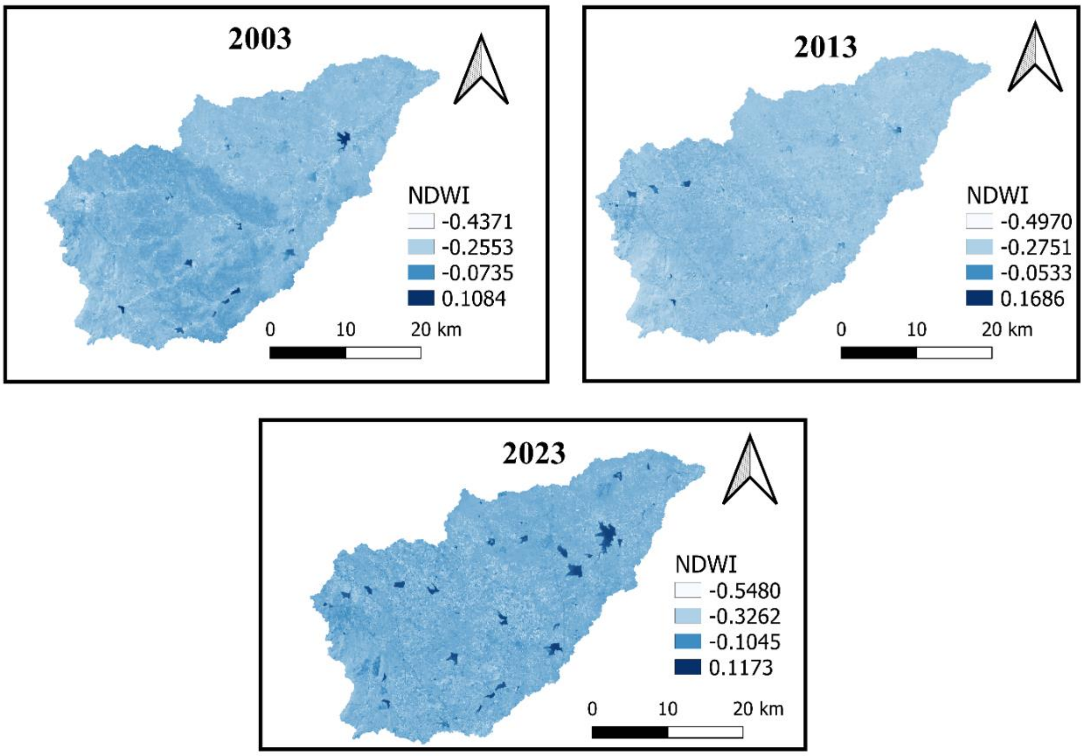

Fig. 4.14 Temporal Variation of NDWI Maps of 2003, 2013 and 2023

4.8 Kappa Accuracy

The LULC classifications in 2003, 2013 and 2023 were found to have Kappa accuracy ratings of 66.58%, 87% and 95% (Fig. 4.15), respectively. These numbers show how classification accuracy had increased steadily over time, reflecting improvements in data quality, remote sensing methods and classification algorithms. The huge improvement in Kappa accuracy over the ten-year period from 2003 to 2013 (66.58% to 87%) pointed to major improvements in LULC categorization approaches. The availability of higher-resolution satellite images, improved classification algorithms and the incorporation of auxiliary data sources might be credited with this improvement.

Additionally, the Kappa accuracy of 95% attained in 2023 denoted a highly accurate LULC classification, highlighting the ongoing maturation and advancement of classification algorithms. This accomplishment highlighted how well the selected approach effectively captures the complex and dynamic nature of land use and land cover. A Kappa coefficient of 91% was obtained from comparing the real LULC classes in 2023 to the simulated classes. This high level of agreement between the observed and simulated classifications pointed to the simulation model's success in simulating the LULC patterns using the data at hand and the applicable classification approach.

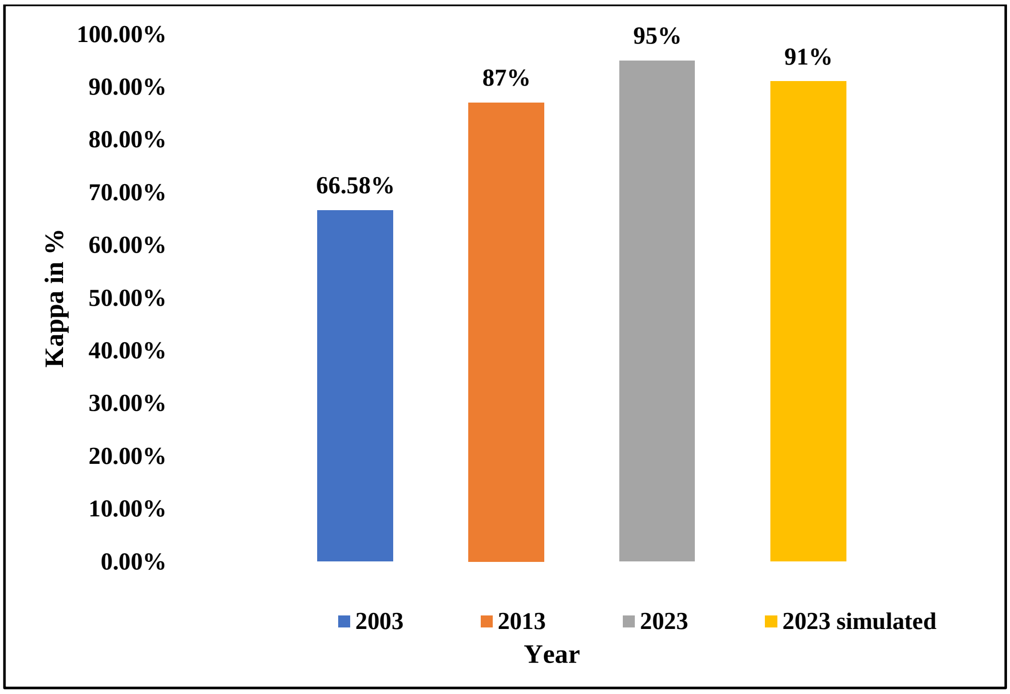

Fig. 4.15 Graph representing Kappa accuracy

Summary and Conclusion

Chapter 5 SUMMARY AND CONCLUSION

The study focused on analyzing the distribution and changes in different land cover classes within the Doddahalla watershed over a 20-year period. Land use and land cover (LULC) patterns for the years 2003, 2013, and 2023 were examined, revealing significant variations in the amounts of forest, urban, fallow, water, agricultural, and barren land and the findings of the study indicated a steady decline in forest area over the past two decades. From 116.79 sq km^2 in 2003, the forest coverage reduced to 55.26 km^2 in 2023, highlighting the significant loss of forested land within the watershed.

On the other hand, agricultural land experienced substantial growth throughout the study period. The agricultural area expanded from 269.12 km^2 in 2003 to 487.82 km^2 in 2023, indicating a significant increase in agricultural activities and land conversion for farming purposes. The extent of fallow land also demonstrated notable changes during the 20-year span. It increased from 360.33 km^2 in 2003 to 488.19 km^2 in 2013, but slightly decreased to 380.73 km^2 in 2023, indicating fluctuations in land use and management practices within the watershed. The study revealed significant changes in the built-up areas of the watershed. The built-up land area, driven by human settlement and infrastructure development, expanded from 16.14 km^2 in 2003 to 72.95 km^2 in 2023, illustrating the rapid urbanization and growth of built infrastructure in the region.

Water bodies within the Doddahalla watershed experienced fluctuations in coverage. Initially, a decline in water area was observed in 2003 due to prolonged drought conditions. However, there was a partial recovery in 2013, followed by another decline in 2023, highlighting the complex interplay of natural factors and potential human-induced impacts on water resources. The conversion of unproductive land into other land use categories, such as agricultural and urban areas, was evident in the study. The area of unproductive land decreased significantly from 319.75 km^2 in 2003 to 70.19 km^2 in 2023, indicating the transformation of this land for more productive purposes. Additionally, the study utilized a CA-Markov prediction model to anticipate future scenarios for the year 2033, particularly focusing on changes in the built-up category induced by recently constructed highways. This analysis highlighted the spatial dispersion of urban areas and their potential impact on land cover dynamics.

Despite the challenges posed by complex land dynamics and data uncertainties, a neural network prediction model demonstrated promising results in predicting LULC classes with an accuracy rate of 63.49%, showcasing the potential of advanced modeling techniques in understanding and forecasting land cover changes.

Moreover, insights into vegetation cover, density, and health were obtained through the analysis of NDVI values derived from Landsat data. The findings revealed improvements in vegetation health and persistent vegetation cover in the Doddahalla watershed over the 20-year period, indicating the importance of preserving and managing green areas. In terms of water bodies, the analysis of NDWI values from Landsat images indicated changes in their extent over the 20-year period. The results predicted a decline in water coverage by 2023, suggesting the need for effective water resource management strategies in the watershed. Overall, the study provides comprehensive insights into the dynamics of land cover and land use in the Doddahalla watershed. The findings highlighted the importance of monitoring and managing these changes to ensure sustainable land use practices, preserve ecosystems, and address environmental challenges in the region.

Conclusions

- The Doodahalla watershed was delineated which gave a geographical boundary to manage the land use and land cover over the region effectively.
- Over the 20-year period, the study area experienced significant transformations in land use, with expansions in agricultural and built-up areas, decreases in forest and water bodies, and the dominance of fallow land as the largest land use category.
- The observed continuous decrease in forest area within the Doddahalla watershed over the study period highlighted the urgent need for conservation efforts to mitigate the ecological impact and preserve the region's diverse flora and fauna.

- The observed expansion of the agricultural land within the Doddahalla watershed highlights the region's thriving agricultural activities, showcasing the positive impact on the local economy and emphasizing the significance of agriculture in the area.
- The observed fluctuation in fallow land area within the Doddahalla watershed suggested potential shifts in land management techniques and agricultural practices over the study period, highlighting the dynamic nature of land use patterns in the region.
- The relentless expansion of the built-up area, caused by population growth and urbanization, underscores the increasing demands and development activities within the study area, highlighting the ongoing transformation of the landscape to accommodate human settlements and infrastructure needs.
- The study demonstrated the resilience of the Doddahalla watershed in recovering water resources following a severe drought, while also indicating the need for further investigation into the factors influencing the observed fluctuations in water area, including ecological conditions and potential human interventions.
- The observed decline in barren land over the study period highlights the dynamic nature of land use in the Doddahalla watershed, with the transformation of unproductive land into productive categories contributing to the overall changes in the region's landscape.
- The study highlighted the need for effective land management strategies and sustainable urban planning to address the environmental and socio-economic challenges associated with rapid urbanization in the Doddahalla watershed of Chitradurga district.
- From 2003 to 2023, NDVI readings in the Doddahalla watershed ranged from -0.14 to 0.51, indicating plant cover. To maintain ecosystem services and environmental health, these regions must be preserved and managed.

- The Doddahalla watershed's NDBI values ranged from -0.31 to 0.55 from 2003 to 2023, indicating a steady urbanisation and built-up area expansion tendency. Efficient land management and sustainable urban planning are needed to overcome the environmental and socio-economic impacts of growing urbanisation.
- NDWI measurements from 2003 to 2023 in the Doddahalla watershed showed changes in water body extent and distribution, ranging from -0.49 to 0.12. Watershed water resource management was needed because water coverage was decreasing. Water resource planning and conservation require hydrological dynamics and water body monitoring.
- The increasing accuracy of LULC classifications demonstrated the progress made in remote sensing techniques and classification algorithms, enabling more reliable monitoring and understanding of land use and land cover dynamics, ultimately supporting informed decision-making and effective land management strategies.

Literature Cited

Adepoju, K.A. and Salami, A.T. 2017. Geospatial assessment of forest fragmentation and its implications for ecological processes in tropical forests. *J. Landsc. Ecol.*, 10(2):19-34.

Agdas, M. G. and Yenen, Z. 2023. Determining land use/land cover (LULC) changes using remote sensing method in Luleburgaz and LULC change's impacts on SDGs. *Eur. J. Sustain. Dev.*, 12(1): 12-45.

Ahmad, M. N., Shao, Z. and Javed, A. 2022. Modelling land use/land cover (LULC) change dynamics, future prospects and its environmental impacts based on geospatial data models and remote sensing data. *Environ. Sci. Pollut. Res.*, 5(1): 42-48.

Ahmed, B. and Ahmed, R. 2012. Modeling urban land cover growth dynamics using multi-temporal satellite images: a case study of Dhaka, Bangladesh. *Int. J. Geo Inf.*, 1(1): 3-31.

Ait El Haj, F., Ouadif, L. and Akhssas, A. 2023. Simulating and predicting future land-use/land cover trends using CA- Markov and LCM models. *Case Stud. Chem. Environ.*, *7*: 322-356.

Aksoy, H. and Kaptan, S. 2021. Monitoring of land use/land cover changes using GIS and CA-Markov modeling techniques: a study in Northern Turkey. *Environ. Monit. Assess.*, 193(8): 98-112.

Aliani, H., Malmir, M., Sourodi, M. and Kafaky, S. B. 2019. Change detection and prediction of urban land use changes by CA-Markov model (case study: Talesh County). *Environ. Earth Sci.*, 78(17): 21-37.

Ambarwulan, W., Syetiawan, A., Rahadiati, A. and Rahmawan, G. A. 2022. Monitoring thirty years of LULC change (1990-2021) from Landsat images of JATABEK, Indonesia. *Earth Environ. Sci.*, 1109(1): 1-9.

Amgoth, A., Rani, H. P. and Jayakumar, K. V. 2023. Exploring LULC changes in Pakhal Lake area, Telangana, India using QGIS MOLUSCE plugin. *Spat. Inf. Res.*, 11(2): 65-73.

Baqa, M. F., Chen, F., Lu, L., Qureshi, S., Tariq, A., Wang, S., Jing, L., Hamza, S. and Li, Q. 2021. Monitoring and modeling the patterns and trends of urban growth using urban sprawl matrix and CA-Markov model: A case study of Karachi, Pakistan. *Land*, 10(7): 1-17.

Behera, M. D., Borate, S. N., Panda, S. N., Behera, P. R. and Roy, P. S. 2012. Modelling and analyzing the watershed dynamics using Cellular Automata (CA)-Markov model-A geo-information-based approach. *Environ. Monit. Assess.*, 19(2): 76-82.

Binh, N. A., Nhut, H. S., An, N. N., Phuong, T. A., Hanh, N. C., Thao, G. T. P., Pham, T. T., Hong, P. V., Ha, L. T. T., Bui, D. T. and Hoa, P. V. 2021. Thirty-year dynamics of LULC at the Dong Thap Muoi area, Southern Vietnam, using Google Earth Engine. *Int. J. Geoinf.*, 10(4): 1-21.

Blaschke, T. 2010. Object based image analysis for remote sensing. *J. Photogramm. Remote Sens.*, 65: 2-16.

Chen, J., Jonsson, P., Tamura, M., Gu, Z., Matsushita, B. and Eklundh, L. 2004. A simple method for reconstructing a high-quality NDVI time-series data set based on the Savitzky-Golay filter. *Remote Sens. Environ.*, 91(34): 332-344.

Disperati, L. and Virdis, S. G. P. 2015. Assessment of land-use and land cover changes from 1965 to 2014 in Tam Giang-CauHai Lagoon, Central Vietnam. *Appl. Geogr.*, 58: 48-64.

Fichera, C. R., Modica, G. and Pollino, M. 2012. Land cover classification and change-detection analysis using multi-temporal remote sensed imagery and landscape metrics. *Eur. J. Remote Sens.*, 45: 1-18.

Flanders, D., Hall-Beyer, M. and Pereverzoff, J. 2003. Preliminary evaluation of eCognition object-based software for cut block delineation and feature extraction. *Can. J. Remote Sens.*, 29(4): 441-452.

Floreano, I. X. and Moraes, L. A. F. 2021. Land use/land cover (LULC) analysis (2009-2019) with Google Earth Engine and 2030 prediction using Markov-CA in the Rondônia State, Brazil. *Environ. Monit. Assess.*, 193(4): 1-17.

Frimpong, B. F., Koranteng, A., Atta-Darkwa, T., Junior, O. F. and Zawiła-Niedzwiecki, T. 2023. Land Cover Changes Utilising Landsat Satellite Imageries for the Kumasi Metropolis and Its Adjoining Municipalities in Ghana (1986–2022). *Sensors, 23*(5): 34-98.

Gandhi, G. M., Parthiban, S., Thummalu, N. and Christy, A. 2015. NDVI: Vegetation change detection using remote sensing and GIS - A case study of Vellore district. *Procedia Comput. Sci.*, 57: 1199-1210.

Gaur, S. and Singh, R. 2023. A comprehensive review on land use/land cover (LULC) change modeling for urban development: current status and future prospects. *Sustainability*, 15(2): 903.

Ghasempour, F., Sekertekin, A. and Kutoglu, S. H. 2023. How Landsat 9 is superior to landsat 8: comparative assessment of land use land cover classification and land surface temperature. *'In: GeoSpatial Conference 2022'* 1(1): 19-22.

Grecchi, R. C., Gwyn, Q. H. J., Benie, G. B., Formaggio, A. B. and Fahl, F. C. 2014. Land use and land cover changes in the Brazilian Cerrado: a multidisciplinary approach to assess the impacts of agricultural expansion. *Appl. Geogr.*, 55: 300-312.

Gulati, A. and Rai, S. C. 2015. Farmers' willingness-to-pay towards soil and water conservation measures in agroecosystems of Chotanagpur Plateau India. *Water Environ. J., 29*(4): 523–532.

Halmy, M. W. A., Gessler, P. E., Hicke, J. A. and Salem, B. B. 2015. Land use/land cover change detection and prediction in the north-western coastal desert of Egypt using Markov-CA. *Appl. Geogr.*, 63: 101-112.

Hamad, R., Balzter, H. and Kolo, K. 2018. Predicting land use/land cover changes using a CA-Markov model under two different scenarios. *Sustainability*, 10: 1-23.

Haque, I. 2021. Monitoring the complex dynamics of LULC change of Tanguar Haor, a Ramsar site in the Northeastern part of Bangladesh *Ecol. Environ. Conserv*.,8(4): 32-98.

He, C., Wang, Y., Zhang, Y. and Hu, Y. 2018. A C-Markov cellular automata model for urban land use change simulation: A case study of Wuhan, China. *Appl. Geogr.*, 91: 32-42.

Huang, S., Tang, L., Hupy, J. P., Wang, Y. and Shao, G. 2021. A commentary review on the use of normalized difference vegetation index (NDVI) in the era of popular remote sensing. In *J. For. Res.* Vol. 32: 23-43.

Ibrahim-Bathis, K., Ahmed, S. A., Govind, R. and Jayakumar, P. D. 2015. Spatio-temporal LULC assessment of Doddahalla watershed of Chitradurga district using remote sensing and GIS Earth resources assessment and management. *Remote Sens. Earth Syst. Sci.*, 28: 1-12.

Ichii, K., Kawabata, A. and Yamaguchi, Y. 2002. Global correlation analysis for NDVI and climatic variables and NDVI trends: 1982-1990. *Int. J. Remote Sens.*, 23(18): 3873-3878.

Irons, J. R., Dwyer, J. L. and Barsi, J. A. 2012. The next Landsat satellite: The Landsat Data Continuity Mission. *Remote Sens. Environ*., 122: 11-21.

Jia, K., Xiangqin, W., Xingfa, G., Yunjun, Y., Xianhong, X. and Bin, L. 2014. Land cover classification using Landsat 8 operational land imager data in Beijing, China. *Geocarto Int.*, 29(8): 941-951.

Jiang, Z., Huete, A. R., Chen, J., Chen, Y., Li, J., Yan, G. and Zhang, X. 2006. Analysis of NDVI and scaled difference vegetation index retrievals of vegetation fraction. *Remote Sens. Environ.*, 101(3): 366-378.

Jokar Arsanjani, J.; Helbich, M.; Kainz, W.; Darvishi Boloorani, (2013). A. Integration of Logistic Regression, Markov Chain and Cellular Automata Models to Simulate Urban Expansion. *Int. J. Appl. Earth Obs. Geoinf. 21*: 265-275.

Kamaraj, M. and Rangarajan, S. (2022). Predicting the future land use and land cover changes for Bhavani basin, Tamil Nadu, India, using QGIS MOLUSCE plugin *Environ. Sci. Pollut. Res.*, 2(1): 1-12.

Khwarahm, N. R., Qader, S., Ararat, K. and Fadhil Al-Quraishi, A. M. 2021. Predicting and mapping land cover/land use changes in Erbil /Iraq using CA-Markov synergy model. *Earth Sci. Inform.*, 14(1): 393-406.

Kshetri, T. B. 2018. Land Use/Land Cover Map of Pokhara: 2018 View project Volume II Geomatics for Sustainable Development NDVI, NDBI AND NDWI calculation using landsat 7 and 8. *Geomat. Sustain. Dev*., 32(21): 245-545.

Liping, C., Yujun, S. and Saeed, S. 2018. Monitoring and predicting land use and land cover changes using remote sensing and GIS techniques-A case study of a hilly area, Jiangle, China. 13(7): 232-453.

Liu, C., Li, W., Zhu, G., Zhou, H., Yan, H. and Xue, P. 2020. Land use/land cover changes and their driving factors in the Northeastern Tibetan Plateau based on geographical detectors and Google Earth Engine: A case study in Gannan Prefecture. *Remote Sens.*, 12(19): 1-18.

Liu, T. and Yang, X. 2015. Monitoring land changes in an urban area using satellite imagery, GIS and landscape metrics. *Appl. Geogr.*, 56: 42-54.

Liu, Y., Wang, Z. and Li, W. 2017. A cellular automata and Markov chain-based land use and land cover change simulation model. *Int. J. Geogr. Inf. Syst.*, 31(4): 704-724.

Loukika, K. N., Keesara, V. R., Buri, E. S. and Sridhar, V. 2022. Predicting the effects of land use land cover and climate change on Munneru River Basin using CA-Markov and soil and water assessment tool. *Sustainability*, 14(9): 1-28.

Maruf, J. K., Ara, S., Bazar, B. and Khalid Maruf, J. 2023. Examining the Spatio-temporal changes of Ecosystem Service Value Due to LULC changes: A Case Study on Cox's Bazar, Bangladesh Examining the Spatio-temporal changes of Ecosystem Service Value Due to LULC changes: A Case Study on Cox's Sustainable development. *Remote Sens. Earth Syst. Sci.*, 12: 5-22.

Mathewos, M., Lencha, S. M. and Tsegaye, M. 2022. Land use and land cover change assessment and future predictions in the Matenchose Watershed, Rift Valley Basin, using CA-Markov simulation. *Land*, 11(10): 1-28.

Mekonnen, Y. and Ghosh, S. K. 2017. Monitoring urban growth and land use/cover changes using remote sensing and geospatial techniques in Adama, Ethiopia. In *An Int. J., (ESTIJ* (Vol. 7, Issue 2), 22(13):1-9.

Modica, G., Vizzari, M., Pollino, M., Fichera, C. R. R., Zoccali, P. and Di-Fazio, S. 2012. Spatio-temporal analysis of the urban–rural gradient structure: An application in a Mediterranean mountainous landscape (Serra San Bruno, Italy). *Earth Syst. Dyn.*, 3: 263-279.

Mohamed, A. and Worku, H. 2020. Simulating urban land use and cover dynamics using cellular automata and Markov chain approach in Addis Ababa and the surrounding. *Urban Climate*, 31: 33-96.

Mondal, M. S., Sharma, N., Garg, P. K. and Kappas, M. 2016. Statistical independence test and validation of CA Markov land use land cover (LULC) prediction results. *Egypt. J. Remote Sens. Space Sci.*, 19(2): 259-272.

Mukhopadhaya, S. 2016. Land use and land cover change modelling using CA-Markov case study: Deforestation analysis of Doon valley. In *J. Agroecol. Nat. Resour.*, 16(3): 10-16.

Nair, A.K.S., Sankar, G. and Kumar, S.N., 1993. Remote Sensing application study of irrigation and offset of coastal Inlets. *J. Indian Soc. Remote Sens*, 21(3): 51-54.

Nasiri, V., Deljouei, A., Moradi, F., Sadeghi, S. M. M. and Borz, S. A. 2022. Land use and land cover mapping using Sentinel-2, Landsat-8 satellite images and Google Earth Engine: A comparison of two composition methods. *Remote Sens.*, 14(9): 1-18.

Omuto, C. T., Vargas, R. R., Alim, M. S. and Paron, P. 2010. Mixed-effects modelling of time series NDVI-rainfall relationship for detecting human-induced loss of vegetation cover in drylands. *J. Arid Environ.*, 74: 1552-1563.

Özelkan, E. 2020. Water body detection analysis using NDWI indices derived from landsat-8 OLI. *Pol. J. Environ. Stud.*, 29(2): 1759-1769.

Padoch, C., Brondizio, E., Costa, S., Pinedo-Vasquez, M., Sears, R. R. and Siqueria, A. 2008. Urban forest and rural cities: multi-sited households, consumption patterns and forest resources in Amazonia. *Ecol. Soc*., 13: 1-23.

Potapov, P. V., Turubanova, S. A., Hansen, M. C., Adusei, B., Broich, M., Altstatt, A., Mane, L. and Justice, C. O. 2012. Quantifying forest cover loss in Democratic Republic of the Congo, 2000–2010, with Landsat ETMþdata. *Remote Sens Environ.*, 122: 106-116.

Pourghasemi, H. R., Moradi, H. R., Fatemi Aghda, S. M. 2013. Landslide susceptibility mapping by binary logistic regression, analytical hierarchy process and statistical index models and assessment of their performances. *Nat. Hazards.*, 69(1): 749-779.

Prawin, B., Masilamani, P. and Rahaman, S. A. 2021. Performance assessment of classification algorithms for landuse / landcover change using sentinel 2 data - A case study of Tiruppur. *'In: American Society for Photogrammetry and Remote Sensing Annual Conference 2021'* at Denver, during. February 6-8. pp 139-142.

Rahnama, M. R. 2021. Forecasting land-use changes in Mashhad Metropolitan area using Cellular Automata and Markov chain model for 2016-2030. In *Sustainable Cities and Society* (Vol. 64). Elsevier Ltd. 5: 141-177.

Rawat, J. S., Biswas, V. and Kumar, M. 2013. Changes in land use/cover using geospatial techniques: A case study of Ramnagar town area, district Nainital, Uttarakhand, India. *Egypt. J. Remote Sens. Sp. Sci*., 2: 111-117.

Regassa, B., Kassaw, M. and Bagyaraj, M. 2020. Analysis of urban expansion and modeling of LULC changes using geospatial techniques: The case of Adama city. *Remote Sens.*4(3): 40-58.

Ridho-Fariz, T. and Nurhidayati, E. 2020. Mapping land coverage in the Kapuas Watershed using machine learning in Google Earth Engine. *J. Appl. Geosp. Info.*, 4(2): 390-395.

Roth, D., Moreno-Sanchez, R., Torres-Rojo, J. M. and Moreno-Sanchez, F. 2016. Estimation of human-induced disturbance of the environment associated with 2002, 2008 and 2013 land use/cover patterns in Mexico. *Appl. Geogr.*, 66: 22-34.

Rulinda, C. M., Dilo, A., Bijker, W. and Stein, A. 2012. Characterising and quantifying vegetative drought in East Africa using fuzzy modelling and NDVI data. *J. Arid. Environ.*, 78: 169-178.

Saah, D., Tenneson, K., Matin, M., Uddin, K., Cutter, P., Poortinga, A., Nguyen, Q. H., Patterson, M., Johnson, G., Markert, K., Flores, A., Anderson, E., Weigel, A., Ellenberg, W. L., Bhargava, R., Aekakkararungroj, A., Bhandari, B., Khanal, N., Housman, I. W. and Chishtie, F. 2019. Land cover mapping in Data Scarce Environments: Challenges and Opportunities. *Int. J. Appl. Earth Obs. Geoinformation*, 85: 1-18.

Schulz, J.J., Cayuela, L., Rey-Benayas, J.M. and Schroder, B. 2011. Factors influencing vegetation cover change in Mediterranean Central Chile (1975–2008). *Appl. Veg. Sci*, 14(4): 1-12.

Setiawan, O. and Nandini, R. 2022. Integration of LULC change/prediction and hydrological modeler for assessment of the effect of LULC Change on peak discharge in Sari Watershed, Sumbawa Island, Indonesia. *IOP Conf. Ser.: Earth Environ. Sci.,1109*(1):57-68

Singh, S. K., Mustak, S., Srivastava, P. K., Szabó, S. and Islam, T. 2015. Predicting spatial and decadal LULC changes through Cellular Automata Markov Chain Models using earth observation datasets and geo-information. *Environ. Process.*, 2(1): 61-78.

Solano, F., Di. Fazio, S. and Modica, G. A. 2019. Methodology based on GEOBIA and WorldView-3 imagery to derive vegetation indices at tree crown detail in olive orchards. *Int. J. Appl*. Earth *Obs. Geoinf.*, 83: 1-20.

Srivastava, A., Bharadwaj, S., Dubey, R., Sharma, V. B. and Biswas, S. 2022. Mapping vegetation and measuring the performance of machine learning algorithm in LULC classification in the large area using sentinel-2 and landsat-8 datasets of Dehradun as a test case. *Int. Arch. Photogramm. Remote Sens.*, 43: 529-535.

Subedi, A. and Dev Acharya, T. 2021. Small Water Bodies Detection and Evaluation using Normalized Difference Water Index (NDWI) from Landsat Image in Western Terai. *Remote Sens. Environ.*, 91(34): 332-344.

Sujarwo, M. W., Hakim, F. L. and Indarto, I. 2023. Using Landsat to track land use and land cover (LULC) change from 1970 to 2020 in Mayang Watershed, East Jawa. *'In: The 5th International Conference on Agriculture and Life Science 2021'* at Jember, during. November 3-4. pp 1-8.

Sundara, K., Udaya, B.P. and Padma Kumari, K. 2015. Application of land change modeler for prediction of future land use land cover a case study of Vijayawada *Int. J. Adv. Technol. Eng. Sci*, 3(1): 34-49.

Tadese, S., Soromessa, T. and Bekele, T. 2021. Analysis of the Current and Future Prediction of Land Use/Land Cover Change Using Remote Sensing and the CA-Markov Model in Majang Forest Biosphere Reserves of Gambella, Southwestern Ethiopia. *Sci. World J.,*4(7): 23-76.

Tariq, A. and Mumtaz, F. 2023. A series of spatio-temporal analyses and predicting modeling of land use and land cover changes using an integrated Markov chain and cellular automata models. *Environ. Sci. Pollut. Res.*3(5): 43-98.

Tassi, A., Gigante, D., Modica, G., di Martino, L. and Vizzari, M. 2021. Pixel- vs. Object-Based Landsat 8 Data classification in Google Earth Engine using random forest: The case study of Maiella National Park. *Remote Sens.*, 13(12): 1-20.

Tassi, A., Gil, A. and Rao, Q. 2020. Diversity Index-based application for detecting, assessing and monitoring coastal land-cover/land-use changes at High Spatial Resolution. *J. Coast. Res*., 95: 1315-1319.

Thapa, R. and Bahuguna, V. 2021. Monitoring land encroachment and land use and land cover (LULC) change in the Pachhua Dun, Dehradun district using Landsat images 1989 and 2020. *Geo. Spat. Inf. Sci.*, 4(1): 71-80.

Twisa, S. and Buchroithner, M. F. 2019. Land-use and land-cover (LULC) change detection in Wami river basin, Tanzania. *Land*, 8: 1-15.

Vizzari, M. and Sigura, M. **2015.** Landscape sequences along the urban–rural–natural gradient: A novel geospatial approach for identification and analysis. *Landsc. Urban Plan.*, 140: 42-55.

Vizzari, M., Hilal, M., Sigura, M., Antognelli, S. and Joly, D. 2018. Urban-rural-natural gradient analysis with CORINE data: An application to the metropolitan France. *Landsc. Urban Plan.*, 171: 18-29.

Yang, J., Chen, F., Xie, P., Su, J. and Ge, Q. 2016. A local land use competition cellular automata model and its application. *Int. J. Geo Inf.*, 5(7): 106.

Yang, X., Zheng, X. and Chen, R. 2014. A land use change model: Integrating landscape pattern indexes and Markov- CA. *Ecol. Model.*, 283: 1-7.

Yasin, M. Y., Abdullah, J., Noor, N. M., Yusoff, M. M. and Noor, N. M. 2022. Landsat observation of urban growth and land use change using NDVI and NDBI analysis. *IOP Conference Series: Earth and Environmental Science, 1067*(1): 1024-1340.

You, H., Tang, X., Deng, W., Song, H., Wang, Y. and Chen, J. 2022. A study on the difference of LULC classification results based on Landsat 8 and Landsat 9 data. *Sustainability*, 14(21): 1-24.

Zhang, C. and Li, X. 2022. Land use and land cover mapping in the era of big data. *Land*, 11(10): 1-22.

CURRICULUM VITAE

Name	:	Dheerajkumar S Hanamapure	**Phone Number**	:	6362836100
Mailing Address	:	C/o Mahantesh Telsang, #349 Bharathi Nagar, 1st Floor Friends Colony, Dharwad, Karnataka 580008	**Permanent Address**	:	Same as mailing address
E-mail	:	hanamapured@gmail.com			

Career objectives : To work in progressive organization where I can continuously learn to achieve functional excellence while making positive contribution to organization.

Educational Qualification

Sr. No.	Examination Passed	Institution	Year	Percentage/ CGPA
1.	Post graduation	G.B.P.U.A& T., Pantnagar Uttarakhand	2023	Pursuing
2.	Graduation	University of Agricultural Sciences Raichur, College of Agricultural Engineering, Raichur Karnataka	2021	79.54 %
3.	Intermediate	J.A. Composite Pre-University College Athani Belgaum Karnataka	2017	68.83 %
4.	High School	Jadhawagi Education Society English Medium High School, Athani, Belgaum, Karnataka	2015	89.92%

Specialization: Agricultural Engineering

Major: Soil and Water Conservation engineering **Minor:** Nil

Thesis Title: ''Cellular Automata and Markov Chain Modelling for Prediction of Future LULC: A Case Study of Doddahalla Watershed in Southern Karnataka''

Conference/Seminars/Workshops/Training Attended: 1

Software Skills: MS Office, Q-GIS, ArcGIS, Google Earth Engine and TerrSet.

Professional Skills: Nil

Professional Affiliations (Membership, etc.,): Nil

Awards/Honors/Achievements: JRF Qualified

Place: Pantnagar
Date: July, 2023

(Dheerajkumar Sidalingappa Hanamapure)

Name	:	Dheerajkumar Sidalingappa Hanamapure	**Id No.**	:	58198
Sem. & year of admission	:	1^{st}, 2021-22	**Degree**	:	M.Tech.
Deptt.	:	Soil and Water Conservation Engineering			
Major	:	Soil and Water Conservation			
Thesis Title	:	**"Cellular Automata and Markov Chain Modelling for Prediction of Future LULC: A Case Study of Doddahalla Watershed in Southern Karnataka"**			
No. of pages	:	69	**Advisor**	:	Dr. Pankaj Kumar

ABSTRACT

This study presented a comprehensive analysis of the distribution and changes in land cover classes within the Doddahalla watershed over a 20-year period and predicted the future LULC of year 2033 based on past and present LULC. Using land use and land cover patterns for the years 2003, 2013, and 2023, the study revealed significant variations in forest, urban, fallow, water, agricultural, and Barren land. The findings highlighted a steady decline in forest area from 116.8 km^2 in 2003 to 55.26 km^2 in 2023, indicating notable loss of forested land. Conversely, agricultural land witnessed substantial growth, expanding from 269.13 km^2 to 487.82 km^2, reflecting remarkable increased agricultural activities and land conversion for farming. Fallow land exhibited fluctuations, increasing from 360.32 km^2 to 488.41 km^2 in 2013 and then slightly decreasing to 380.73 km^2 in 2023. Built-up areas expanded from 16.14 km^2 to 72.95 km^2, highlighting rapid urbanization and infrastructure development in the study region. Water bodies experienced fluctuations, initially declining in 2003 due to drought, partially recovering in 2013, and declining again in 2023, demonstrating the complex interplay of natural factors and human-induced impacts. Barren land decreased from 319.75 km^2 to 70.19 km^2, indicating its transformation into more productive categories. The CA-Markov prediction model utilized cellular automata principles and Markov chain analysis to forecast land cover changes in the Doddahalla watershed for the year 2033, by incorporating recent construction data and considering the historical patterns of land cover change. A neural network prediction model achieved a 63.49% accuracy rate in predicting future land use and land cover classes, showcasing the effectiveness of these methods in monitoring and forecasting land use patterns. This approach provided valuable insights into the potential impacts of urbanization and infrastructure development on the region's land use and land cover. Also, the Indices for LULC Change Assessment like NDVI, NDWI and NDBI were calculated. Overall, this study provides comprehensive insights into land cover dynamics in the Doddahalla watershed, emphasizing the importance of monitoring and managing these changes for sustainable land use, ecosystem preservation, and addressing environmental challenges.

Keywords: Land cover change, land use, land dynamics, urbanization, future prediction, CA-Markov, Kappa.

(Pankaj Kumar)
Advisor

(Dheerajkumar Sidalingappa Hanamapure)
Author

नाम	:	धीरजकुमार सिद्दालिंगप्पा हनमापुरे	**परिचयांक सं.**	:	58198
सत्र एवं प्रवेश वर्ष	:	प्रथम, 2021-22	**उपाधि**	:	मास्टर ऑफ टेक्नोलॉजी
विभाग	:	मृदा एवं जल संरक्षण अभियात्रिकी			
मुख्य विषय	:	मृदा एवं जल संरक्षण अभियात्रिकी			
थीसिस शीर्षक	:	**"सेल्युलर ऑटोमेटा और मार्कोव श्रृंखला मॉडलिंग द्वारा भविष्य के भूमि उपयोग और आवरण वर्गों का पूर्वानुमान: दक्षिणी कर्नाटक के दोद्दहल्ला वॉटरशेड का एक अध्ययन"**			
पृष्ठ संख्या	:	69	**सलाहकार**	:	डॉ. पंकज कुमार

सारांश

यह अध्ययन दोद्दहल्ला वॉटरशेड के भूमि आवरण वर्गों के वितरण और परिवर्तनों का 20-वर्षीय अवधि के भीतर विस्तृत विश्लेषण प्रस्तुत करता है और पिछले और वर्तमान भूमि आवरण वर्गों पर आधारित वर्ष 2033 के भविष्य LULC का पूर्वानुमान प्रस्तुत किया गया। 2003, 2013 और 2023 के लिए भूमि उपयोग और आवरण वर्गों के पैटर्न का उपयोग किये, इस अध्ययन में वन, शहरी, बंजर, जलीय, कृषि और खाली जमीन की महत्वपूर्ण विभिन्नताओं का विश्लेषण किया गया। अध्ययन के अनुसार 2003 में 116.8 km^2 से 2023 में 55.26 km^2 तक वन क्षेत्र में कमी हुई है, जिससे वन क्षेत्र में कमी की जानकारी मिलती है। इसके विपरीत कृषि की भूमि में बड़ी वृद्धि हुई है, जो 269.13 km^2 से 487.82 km^2 तक फैल गई है, इससे विशेष रूप से कृषि गतिविधियों और खेती के लिए भूमि के परिवर्तन का संकेत मिलता है। 2013 में बंजर जमीन में बदलाव देखा गया, जो 360.32 km^2 से 2013 में 488.41 km^2 तक बढ़ी और फिर 2023 में 380.73 km^2 हो गई। अध्ययन, के अनुसार वाटरशेड क्षेत्र में शहरीकरण और बुनियादी ढांचे के विकास के संकेत के रूप में प्रदर्शित करता है की यहां 16.14 km^2 से 2023 में 72.95 km^2 तक बढ़ गए हैं। जलवायुविज्ञानीय तथा मानव के प्रेरित प्रभावों के जटिल संयोजन का LULC पर स्पष्ट प्रभाव पड़ता है। 319.75 km^2 से 70.19 km^2 तक बंजर जमीन में कमी हुई है, जिससे इसे और उत्पादक श्रेणियों में परिवर्तित होने का संकेत मिलता है। सीए-मार्कोव पूर्वानुमान मॉडल ने सेल्युलर ऑटोमेटा सिद्धांतों और मार्कोव श्रृंखला विश्लेषण का उपयोग किया और वर्ष 2033 के लिए दोद्दहल्ला वॉटरशेड में भूमि आवरण के परिवर्तनों के पूर्वानुमान किए। हाल के निर्माण डेटा को शामिल करने और इतिहासिक भूमि आवरण परिवर्तन का ध्यान रखने से, यह मॉडल इलाके के भविष्य में निर्मित श्रेणी के वितरण के संभावित स्थिति का पूर्वानुमान करता है।

(पंकज कुमार)	**(धीरजकुमार सिद्दालिंगप्पा हनमापुरे)**
सलाहकार	लेखक